

HIGHMMT: Towards Modality and Task Generalization for High-Modality Representation Learning

Paul Pu Liang^{*1}, Yiwei Lyu^{*1}, Xiang Fan¹, Shentong Mo¹,
 Dani Yogatama², Louis-Philippe Morency¹, Ruslan Salakhutdinov¹
¹Carnegie Mellon University, ²DeepMind
 {плианг, ylyu1}@cs.cmu.edu

Abstract

Learning multimodal representations involves discovering correspondences and integrating information from multiple heterogeneous sources of data. While recent research has begun to explore the design of more general-purpose multimodal models (contrary to prior focus on domain and modality-specific architectures), these methods are still largely focused on a small set of modalities in the language, vision, and audio space. In order to accelerate generalization towards diverse and understudied modalities, we investigate methods for high-modality (a large set of diverse modalities) and partially-observable (each task only defined on a small subset of modalities) scenarios. To tackle these challenges, we design a general multimodal model that enables *multitask* and *transfer* learning: multitask learning with shared parameters enables stable parameter counts (addressing scalability), and cross-modal transfer learning enables information sharing across modalities and tasks (addressing partial observability). Our resulting model generalizes across text, image, video, audio, time-series, sensors, tables, and set modalities from different research areas, improves the tradeoff between performance and efficiency, transfers to new modalities and tasks, and reveals surprising insights on the nature of information sharing in multitask models. We release our code and benchmarks which we hope will present a unified platform for subsequent theoretical and empirical analysis: <https://github.com/pliang279/HighMMT>.

1. Introduction

Multimodal machine learning (ML) brings unique challenges for both computational and theoretical research given the heterogeneity of various data sources (Baltrušaitis et al., 2018). Current multimodal ML research has led to impressive advances in modeling for specific domains such as language, vision, and audio understanding (Ledin and Machin, 2020; Ngiam et al., 2011; Agrawal et al., 2017; Ramesh et al., 2021) with applications such as multimedia (Atrey et al., 2010; Shah and Zimmermann, 2017), affective computing (Liang et al., 2019; Poria et al., 2017), and robotics (Kirchner et al., 2019; Lee et al., 2019). However, with advances in sensing technologies, many real-world platforms such as cellphones (Liang et al., 2021a), smart devices (Hamisu et al., 2011), self-driving cars (Yeong et al., 2021), healthcare technologies (Johnson et al., 2016), and robots (Belpaeme et al., 2018; Kim et al., 2013) now integrate a much larger number of sensors beyond the prototypical language, visual, and acoustic modalities. Moving forward, modality and task-specific models may lead to a larger set of architectural decisions and training parameters, risk marginalizing research on relatively understudied

*Equal contribution

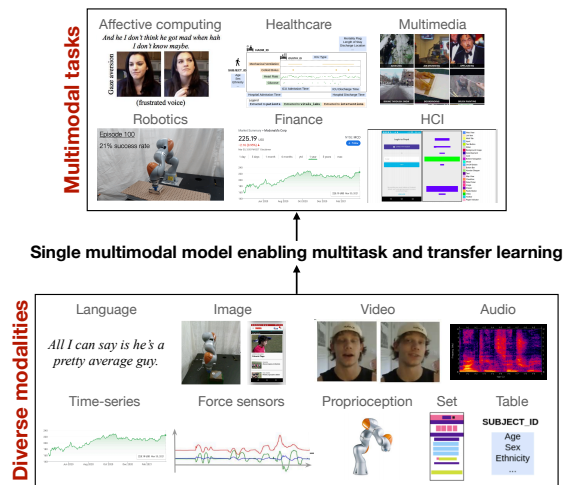


Figure 1. Can we learn a general model for different multimodal tasks, as an alternative to existing modality/task-specific models (Ngiam et al., 2011; Baltrušaitis et al., 2018; Jayakumar et al., 2020; Liang et al., 2021b)? A general model would present computational benefits over separate ones (multitask learning), enable statistical strength sharing (transfer learning), and provide a unified platform for subsequent theoretical and empirical analysis.

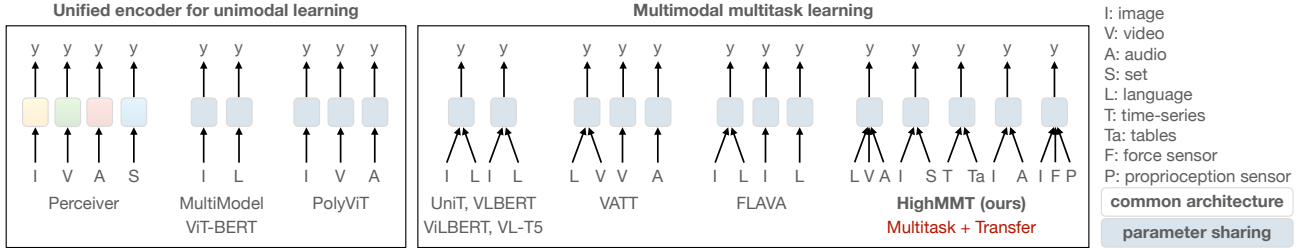


Figure 2. In contrast to current work in unified unimodal encoders (Jaegle et al., 2021b; Kaiser et al., 2017; Li et al., 2021; Likhoshesterov et al., 2022) and multimodal multitask learning (Hu and Singh, 2021; Lu et al., 2019; Su et al., 2020; Cho et al., 2021; Akbari et al., 2021; Singh et al., 2021), we aim to design a general-purpose model for high-modality and partially-observable scenarios, which presents two main technical challenges: (1) *scalability*, since adding new parameters for every new modality/task becomes prohibitively expensive, and (2) *partial observability*, since each task is defined only over a small subset of all modalities we are interested in modeling.

modalities, all while losing out on the advantage of statistical strength sharing across modalities, domains, and tasks. There is therefore a demand for general-purpose models that can handle a large number of modality inputs while also operating on diverse and understudied modalities.

Recent work has explored general-purpose models over two or three modalities, typically in the language, vision, and audio space (Jaegle et al., 2021b; Hu and Singh, 2021; Akbari et al., 2021). To the best of our knowledge, a general-purpose model for multimodal tasks over a larger set of diverse modalities does not yet exist. This new problem statement presents two main technical challenges: (1) *scalability*, since adding new parameters for every new modality or task becomes prohibitively expensive, and (2) *partial observability*, since each task is often defined only over a small subset of all modalities we are interested in modeling.

In this paper, we study the question of designing a general-purpose model for high-modality and partially-observable scenarios (see Figure 1). Key to tackling the aforementioned challenges are *multitask* and *transfer* learning: multitask learning with shared unimodal and multimodal layers enables stable parameter counts (addressing scalability) and cross-modal transfer learning enables information sharing across modalities and tasks (addressing partial observability). However, one would not typically expect the same model (architecture and parameters) to simultaneously encode joint representations between different subsets spanning images, text, audio, sets, time-series, and graphs. Furthermore, multimodal learning paradigms have been vastly different across tasks, spanning Transformers (Tsai et al., 2019; Lu et al., 2019), multiplicative interactions (Jayakumar et al., 2020; Perez et al., 2018), tensors (Liang et al., 2019), and gated units (Chaplot et al., 2018; Wang et al., 2020) (see Liang et al. (2021b) for a categorization).

To answer this question, we build upon the recent promise of general self-attention-based models that can simultaneously encode text (Devlin et al., 2019), images (Dosovitskiy et al., 2021), and audio (Akbari et al., 2021) to design a general

multimodal multitask transformer. We observe that under the right level of parameter sharing and multitask training, it is possible to train a single model that:

- (1) Is suitable for numerous high-modality and partially-observable multimodal tasks (across 10 modalities, 15 prediction tasks, and 5 research areas), achieving strong performance while reducing total parameter counts.
- (2) Enables cross-modal information transfer by pretraining on source multimodal tasks before transferring to completely new target modalities and tasks, with larger improvements for low-resource target tasks.
- (3) Improves the tradeoff between performance and efficiency over task-specific state-of-the-art models especially in low-resource scenarios (less training data and partially-observable modalities).

Beyond these empirical results, we believe that our insights on visualizing and understanding the nature of information sharing, as well as the generalization and regularization effects of multimodal multitask learning, are useful for future work. Our implementations and benchmarks are publicly available which we hope will present a unified platform for subsequent theoretical and empirical analysis.

2. Related Work

Multimodal Transformers have emerged as strong general-purpose models for representation learning. Building upon the initial text-based Transformer model (Vaswani et al., 2017), these multimodal extensions typically use either full self-attention over modalities concatenated across the sequence dimension (Li et al., 2019; Sun et al., 2019; Su et al., 2020; Chen et al., 2020) or a cross-modal attention layer (Lu et al., 2019; Tsai et al., 2019; Tan and Bansal, 2019), and are useful for sequential data by automatically aligning and capturing complementary features at different time-steps (Tsai et al., 2019; Yao and Wan, 2020; Lee et al., 2020c). Self-supervised multimodal pretraining has emerged as an effective way to train these powerful architectures, with the aim of learning general-purpose represen-

tations from larger-scale unlabeled multimodal data before transferring to specific downstream tasks via supervised fine-tuning (Lu et al., 2019; Li et al., 2019; Su et al., 2020). These pretraining objectives typically consist of unimodal masked prediction, crossmodal masked prediction, and multimodal alignment prediction (Hendricks et al., 2021).

Unified encoder for unimodal learning. Several works such as Perceiver (Jaegle et al., 2021a;b), Multi-Model (Kaiser et al., 2017), ViT-BERT (Li et al., 2021), and PolyViT (Likhoshesterov et al., 2022) have explored the possibility of using the same unimodal encoder architecture for different inputs on unimodal tasks (i.e., language, image, video, or audio-only). The Transformer architecture has emerged as a popular choice due to its suitability for serialized inputs such as text (sequence of tokens) (Devlin et al., 2019), images (sequence of patches) (Dosovitskiy et al., 2021), video (sequence of images) (Sun et al., 2019), and other time-series data (sequence of timesteps) (Lim et al., 2021), a phenomenon further observed by Lu et al. (2021) where a single Transformer pretrained on text transfers to other unimodal tasks including sequence modeling and image classification. While these serve as building blocks in our model, our focus is on a general-purpose multimodal model for multitask and transfer learning across different subsets of modalities rather than unimodal tasks. We summarize some of these differences in Figure 2.

Multimodal multitask and transfer learning. There have also been several attempts to build a single model that works well on a suite of multimodal tasks (Li et al., 2019; Lu et al., 2019; Su et al., 2020; Cho et al., 2021). For example, UniT (Hu and Singh, 2021), VLBERT (Su et al., 2020), ViLBERT (Lu et al., 2019), and VL-T5 (Cho et al., 2021) are all unifying models for vision-and-language tasks, with some models also possessing generalization to vision-only and language-only tasks. VATT (Akbari et al., 2021) jointly trains a shared model on video, audio, and text data to perform audio-only, video-only, and image-text retrieval tasks. FLAVA (Singh et al., 2021) found that pretraining a shared model with unpaired images, unpaired text, and image-text pairs results in strong performance on image-only, text-only, and image-text multimodal tasks. On the transfer side, while more research has focused on transfer within the same modality with external information (Socher et al., 2013; Dunnmon et al., 2019; Xing et al., 2019; Zadeh et al., 2020), Liang et al. (2021c) is the only work that studies transfer to completely new modalities. However, they require paired data collection and modality-specific modeling for specific unimodal transfer tasks. Our work goes beyond the commonly studied language, vision, and audio modalities to relatively understudied ones (e.g., tabular data, time-series, sensors, graphs, and set data). Furthermore, we show the possibility of generalizing to new modality subsets using general models, which can further enable quick

generalization to new domains and tasks.

Multimodal benchmarks have emerged as a crucial component testing the generalization of models in multitask and transfer settings. Ideal benchmarks should reflect real-world distribution shifts between multiple diverse tasks and research areas. In language and vision, these have consolidated into a suite of datasets spanning image-text retrieval (Young et al., 2014; Plummer et al., 2015), image-text question answering (Agrawal et al., 2017; Zellers et al., 2019; Kazemzadeh et al., 2014), and image-text fusion (Kiela et al., 2020; Vielzeuf et al., 2018; Kay et al., 2017; Arevalo et al., 2017). Beyond these two modalities, MultiBench is a large-scale benchmark spanning more than 15 modalities and tasks while evaluating generalization, complexity, and robustness (Liang et al., 2021b).

3. HIGHMMT

In this section, we describe our model for high-modality and partially-observable multimodal tasks (illustrated in Figure 3). We call our resulting model HIGH-MODALITY MULTIMODAL TRANSFORMER (HIGHMMT). We describe its key characteristics here and include details in Appendix A.

1. Standardized input sequence. We treat each modality as a sequence of embeddings, as is already done for sequential data such as text, audio, and time-series. For images, we break the image into 3×3 or 4×4 patches and treat it as a sequence of 9/16 image regions (Dosovitskiy et al., 2021). For modalities such as tables, sets, and graphs we treat each element in the table/set/graph as an element in the sequence. The end result is a standardized input data format of dimension $\mathbf{x}_m \in \mathbb{R}^{n \times t_m \times d_m}$, where n is the common batch-size, t_m is a modality and task-specific input sequence length, and d_m is a modality and task-specific input dimension.

2. Modality-specific embedding and positional encoding. For each distinct modality $m \in M$ (which may appear across multiple tasks), we define a one-hot modality embedding $\mathbf{e}_m \in \mathbb{R}^{|M|}$, where $|M|$ is the total number of distinct modalities. This embedding layer identifies common modalities across different tasks to enable sharing of information. For example, the modality embedding of the image sequence for a video classification task will be shared with that for an image and text question-answering task.

We also introduce modality-specific Fourier feature positional encodings $\mathbf{p}_m \in \mathbb{R}^{t_m \times d_{pm}}$, where d_{pm} is the positional encoding dimension, to capture temporal and positional information across each modality. For multimodal tasks where a common dimension is shared across time (e.g., videos and other time-series data in the robotics and finance domains), we apply a common positional encoding to capture the common time dimension (i.e., first image frame occurs at the same time as the first word and first audio segment). Different positional encoding dimensions are applied to 1D and 2D input modalities.

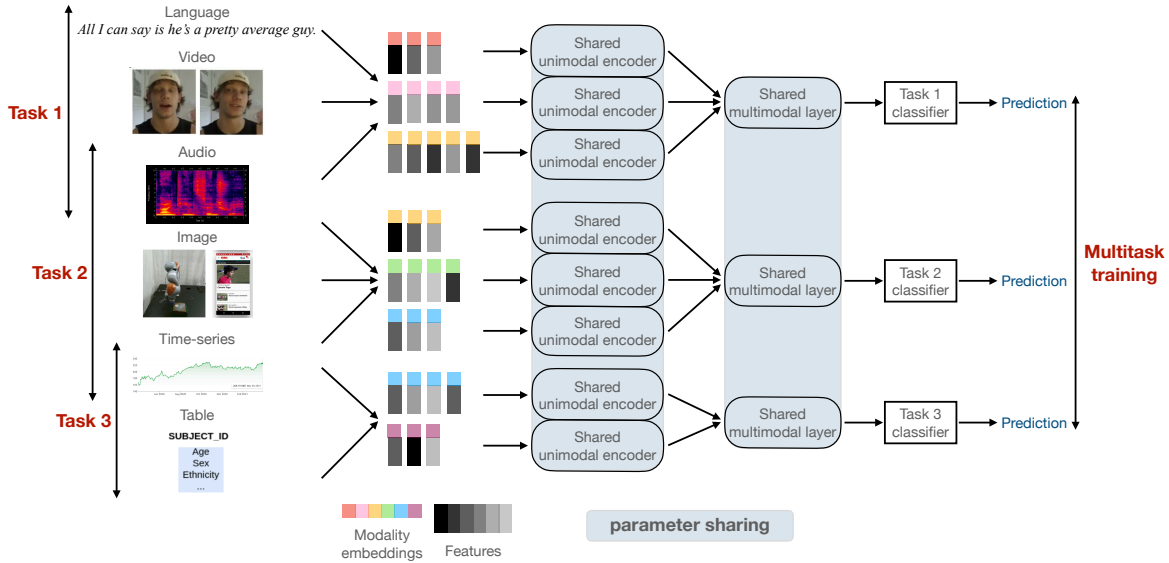


Figure 3. HIGHMMT: our general multimodal model is based on standardizing input modalities into a sequence and using modality-specific embedding layers to capture information unique to each modality. The rest of the model learns modality and task-agnostic representations through shared unimodal encoders and shared multimodal layers trained via multitask learning, which enables statistical strength sharing, parameter efficiency, and quick generalization to new modalities and tasks.

3. Modality and task-agnostic unimodal encoder. Given modality-specific embeddings and positional encodings, the final input representation can now be processed by a general unimodal encoder. We parametrize this general unimodal encoder via multiple layers of a Transformer-based Perceiver block (Jaegle et al., 2021b). The input layer query is first set with a latent $d_{LN} \times d_{LS}$ block, and the context is set as \mathbf{x}_m concatenated with modality embeddings and positional encodings along the last dimension. Consequently, self-attention learns relationships between elements in each modality, resulting in unimodal contextualized representations $\mathbf{z}_m \in \mathbb{R}^{n \times d_{LN} \times d_{LS}}$. Note that only one copy of a unimodal Transformer (Perceiver) block is used to encode all modalities simultaneously, which enables statistical strength sharing and general-purpose representation learning regardless of the specific input modality.

4. Modality and task-agnostic multimodal representation. To learn modality and task-agnostic multimodal representations, we use multiple layers of a general-purpose Crossmodal Transformer block (Tsai et al., 2019; Lu et al., 2019). Given 2 unimodal representations \mathbf{z}_1 and \mathbf{z}_2 , a Crossmodal Transformer (CT) block uses crossmodal self-attention by setting the input layer query $Q = \mathbf{z}_1$ and keys and values $K, V = \mathbf{z}_2$ to learn attention from modality 1 to modality 2, and a separate block to capture the attention in the opposite direction. This step enables one modality’s sequence elements to discover correspondences in another. A Crossmodal Transformer block using \mathbf{z}_1 to attend to \mathbf{z}_2 (and vice-versa) results in a final multimodal representation $\mathbf{z}_{mm} = [\mathbf{z}_{1 \rightarrow 2}, \mathbf{z}_{2 \rightarrow 1}] = [\text{CT}(\mathbf{z}_1, \mathbf{z}_2), \text{CT}(\mathbf{z}_2, \mathbf{z}_1)]$. For tasks with more than 2 modalities, a Crossmodal block is

applied for each pair of modalities before concatenating all multimodal representations. Again, only one copy of a multimodal layer is used on all tasks to learn general representations regardless of the input modalities and task.

5. Task-specific classifier. Finally, on top of concatenated and batch-normalized multimodal representations \mathbf{z}_{mm} , we use a linear classification layer per task for task-specific prediction, where individual correspondences within and across modalities are composed to form a final prediction.

6. Multitask training. To enable information sharing across modalities and tasks, we train across a diverse set of datasets in a multitask manner. While related work has investigated the effect of various multitask training heuristics in detail (Likhoshesterov et al., 2022), we found that optimizing a simple weighted sum of losses over all tasks was sufficient to obtain strong multitask performance.

4. Experiments

In this section, we design experiments to analyze the multitask, transfer, and generalization capabilities of HIGHMMT. We use a large collection of multimodal datasets provided in the standardized and public MultiBench benchmark¹ (Liang et al., 2021b) spanning 15 real-world datasets, 10 modalities, 20 prediction tasks, and 6 research areas. We trained 3 multitask models across combinations of these datasets (see Table 1 and Appendix B for details). Overall, the total size of datasets involved in our experiments exceeds 370,000 and covers diverse modalities such as image, video, audio, text, time-series, various robotics sensors, sets, and tables,

¹<https://github.com/pliang279/MultiBench>

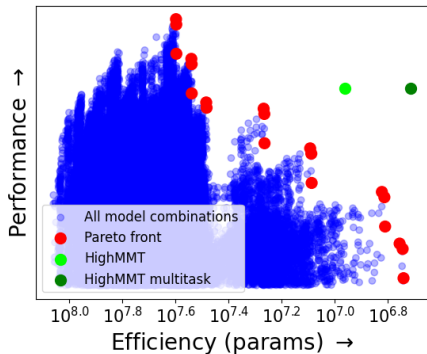


Figure 4. **Overall tradeoff.** Multitask HIGHMMT pushes forward the Pareto front of performance and efficiency as compared to all possible ($> 10^5$) combinations of task-specific models across multiple datasets (Liang et al., 2021b). The x -axis denotes (inverted) total parameters and y -axis denotes performance scaled to a 0 – 1 range before averaging across datasets.

prediction tasks from multimodal fusion to retrieval, as well as multiple research areas spanning affective computing, healthcare, multimedia, robotics, and HCI.

4.1. Multitask performance and efficiency

In Figure 4, we summarize the overall tradeoff between performance and efficiency using a single HIGHMMT model. The blue dots represent all possible combinations of task-specific models across multiple datasets (summarized in MultiBench (Liang et al., 2021b), $> 10^5$ total combinations) with their overall performance (scaled to a 0 – 1 range before averaging across datasets) and overall efficiency (inverted total number of parameters). The red dots represent the state-of-the-art Pareto front: points that are not strictly dominated in both performance and efficiency. In light green, separate single-task HIGHMMT models already improve parameter efficiency due to the sharing of unimodal encoders (within a task only) as compared to standard Multimodal Transformers with modality-specific unimodal encoders (Lu et al., 2019; Tsai et al., 2019). HIGHMMT trained in a multitask manner (dark green), with parameter sharing across unimodal and multimodal layers within and across tasks, further pushes forward the Pareto front by improving both performance and efficiency.

4.2. Generalization to new modalities and tasks

HIGHMMT also offers opportunities to study whether we can *transfer* knowledge between completely different modalities and tasks. On the large setting, we pretrained a model on 1/2/3 of the 4 tasks before fine-tuning on the fourth task only (e.g., train on UR-FUNNY, MOSEI, MIMIC and transfer to AV-MNIST). From Table 2, we found that on all four combinations of multitask pretraining and fine-tuning, weights learned from other multimodal tasks generalize well to new modalities and tasks, improving performance over single target-task training. We further analyze this cross-modal transfer phenomenon by studying the following:

Effect of pretraining datasets. When we increase the number of pretraining datasets, we observe a consistent improvement on fine-tuned target task performance. This effect is particularly pronounced on the UR-FUNNY target task, which shows the biggest improvement using pretrained parameters from 0 to 3 multitask datasets. This implies that HIGHMMT learns more generalizable multimodal features as more tasks are involved in multitask training.

Effect of target dataset size. We observed an inverse correlation between target task size and performance improvement: the smallest dataset, UR-FUNNY, benefited the most (+2.4%) from transfer learning. This implies that our multimodal pretraining-fine-tuning paradigm is useful for low-resource target modalities and tasks.

Effect of transfer modalities. We compare transfer learning performance across different levels of partial observability. While one would expect transfer to MIMIC to be the hardest due to its modality set {time-series, table} being completely disjoint from the remaining 3 datasets, we still observe a +0.8% gain as compared to single-task training. Therefore, HIGHMMT can generalize to new modalities and tasks. Unsurprisingly, for datasets with more overlap (e.g., UR-FUNNY with complete overlap in {text, video, audio} with respect to pretraining), we find larger improvements using transfer learning over single-task models (+2.4%).

4.3. Comparison with task-specific state-of-the-art

In Table 3, we compare multitask performance and efficiency with task-specific state-of-the-art models. We achieve performance within the range of published models (and usually close to the individual task-specific state-of-the-art) in MultiBench (Liang et al., 2021b). In fact, HIGHMMT even sets new state-of-the-art results on several datasets, especially on the relatively understudied modalities (time-series, force and proprioception sensors, and sets) from the robotics (PUSH, V&T) and HCI (ENRICO) research areas. On top of strong performance, the main benefit lies in using fewer total parameters as compared to separate task-specific models - reduction by the number of tasks involved. Since this reduction grows with the number of tasks, our approach is scalable to high-modality scenarios. Finally, multitask HIGHMMT performs similar to (and sometimes better than) its single-task version while reducing parameters.

4.4. Few-shot learning

HIGHMMT offers opportunities for statistical strength sharing across tasks. We test this hypothesis in the few-shot learning scenario, by evaluating whether multitask information sharing can improve performance on low-resource target tasks. We compare a single-task HIGHMMT trained only on a percentage p of labeled training data in the target task with multitask HIGHMMT trained on the same percentage p (during multitask training we prioritize performance

Table 1. We investigate 3 multitask training setups to evaluate the performance of HIGHMMT. Each multitask setup is designed to include tasks with different modality inputs and prediction objectives. The total size of datasets involved in our experiments exceeds 370,000, and covers diverse modalities, prediction tasks, and research areas.

Setting	Datasets	Modalities	Size	Prediction task	Research Area
Small	PUSH	{image, force, proprioception, control}	37,990	object pose	Robotics
	V&T	{image, force, proprioception, depth}	147,000	contact, robot pose	Robotics
Medium	ENRICO	{image, set}	1,460	design interface	HCI
	PUSH	{image, force, proprioception, control}	37,990	object pose	Robotics
	AV-MNIST	{image, audio}	70,000	digit	Multimedia
Large	UR-FUNNY	{text, video, audio}	16,514	humor	Affective Computing
	MOSEI	{text, video, audio}	22,777	sentiment, emotions	Affective Computing
	MIMIC	{time-series, table}	36,212	mortality, ICD-9 codes	Healthcare
	AV-MNIST	{image, audio}	70,000	digit	Multimedia

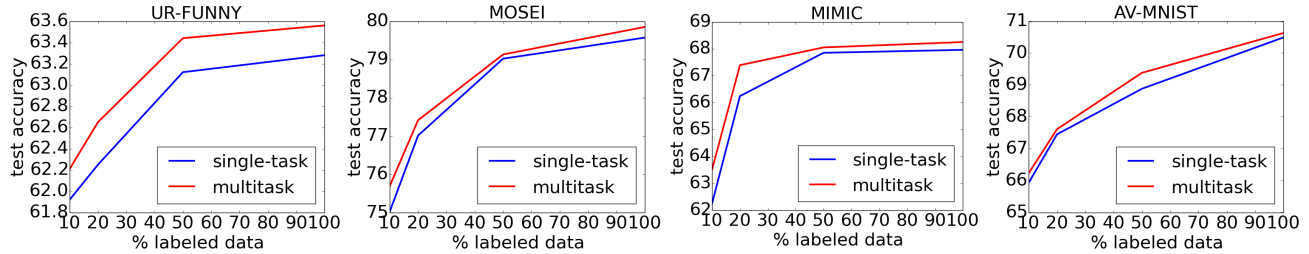


Figure 5. Few-shot results on new modalities and tasks. Multimodal multitask training using HIGHMMT learns more generalizable representations which improves performance across all ranges of data. The x-axis shows percentage of labeled data used during training.

Table 2. Cross-modal transfer to new modalities and tasks. We train multitask HIGHMMT on 1/2/3 datasets and find that it generalizes to new modalities and tasks on the 4th dataset, with improved performance over single-task training on the 4th dataset. Cross-modal transfer improves with the number of pretraining tasks and works best on smallest target tasks (UR-FUNNY).

# Source tasks	Target task			
	UR-FUNNY	MOSEI	MIMIC	AV-MNIST
0 (no transfer)	63.3	79.4	67.7	70.4
1	64.1	79.4	68.3	70.4
2	65.5	80.0	68.5	70.5
3	65.7	80.5	68.5	70.5

of the target task over others). By varying $p \in [0.1, 1.0]$, we plot the performance under few-shot settings in Figure 5. We find that multitask training is consistently better across all ranges of data, which supports the fact that more generalizable representations across modalities and tasks are learned in HIGHMMT. The main takeaway is that if it is too difficult to collect data in a target domain, collecting data from a different domain and using a shared multimodal model is an alternative approach for improving performance.

4.5. Multitask fusion and retrieval

Finally, we perform multitask training over multimodal fusion in AV-MNIST and retrieval in CIFAR-ESC. While fusion emphasizes information integration from complementary data sources, retrieval focuses on aligning corresponding elements expressed through different views of the data (Baltrušaitis et al., 2018). Even across these vastly different prediction tasks, we find that multitask training

(60.5% retrieval accuracy) improves upon single-task training (58.8% retrieval accuracy). Not only have the unimodal encoders simultaneously processed different modalities, the multimodal layer has also learned to capture correspondences useful for both fusion and retrieval.

4.6. Ablation studies

We further analyze each component of HIGHMMT:

1. **HIGHMMT w/o embeddings** removes the only modality-specific component in the model - the modality embeddings. We set embeddings for all modalities to be the same to test whether a modality-specific component is necessary to capture heterogeneity across input data sources.
2. **HIGHMMT w/o unimodal** removes the unimodal encoder and directly applies the cross-attention layer, and **HIGHMMT w/o multimodal** replaces the multimodal cross-attention layer with a concatenation of unimodal features and a linear classification layer. The latter resembles the most direct multimodal extension of existing work in shared unimodal encoders like Perceiver (Jaegle et al., 2021b), MultiModel (Kaiser et al., 2017), ViT-BERT (Li et al., 2021) or PolyViT (Likhoshesterov et al., 2022).
3. **HIGHMMT separate** uses separate unimodal and multimodal layers reminiscent of typical single-task multimodal transformers (Tsai et al., 2019; Lu et al., 2019; Hendricks et al., 2021). **HIGHMMT separate unimodal (multimodal)** only separates the unimodal (multimodal) layer during multitask training.

From Table 4, removing any of the 3 components in HIGH-

Table 3. HIGHMMT achieves strong performance on overall performance and efficiency, sometimes even beating (shown in **bold**) the task-specific state-of-the-art, especially on the relatively understudied modalities (time-series, robotics sensors, and sets) from the robotics (PUSH, V&T) and HCI (ENRICO) research areas. MultiBench range captures the min and max (SOTA) performance and parameters of more than 20 recent multimodal models implemented in Liang et al. (2021b).

Small setting	PUSH ↓	V&T ↑	Params (M) ↓
MultiBench range	0.574 – 0.290	93.3 – 93.6	2.03 – 24.7
MultiBench SOTA	0.290	93.6	2.03
HIGHMMT	0.201	96.5	4.18
HIGHMMT multitask	0.386	96.1	1.00

Medium setting	ENRICO ↑	PUSH ↓	AV-MNIST ↑	Params (M) ↓
MultiBench range	44.4 – 51.0	0.574 – 0.290	65.1 – 72.8	21.2 – 51.7
MultiBench SOTA	51.0	0.290	72.8	21.30
HIGHMMT	52.6	0.278	70.4	2.91
HIGHMMT multitask	53.1	0.287	70.4	0.93

Large setting	UR-FUNNY ↑	MOSEI ↑	MIMIC ↑	AV-MNIST ↑	Params (M) ↓
MultiBench range	58.3 – 66.7	76.4 – 82.1	67.6 – 68.9	65.1 – 72.8	0.41 – 37.7
MultiBench SOTA	66.7	82.1	68.9	72.8	9.86
HIGHMMT	63.3	79.4	67.7	70.4	2.11
HIGHMMT multitask	63.0	79.9	67.8	70.4	0.53

Table 4. **Ablation studies** show that removing any of the 3 components in HIGHMMT results in worse overall performance, and separating rather than sharing parameters also reduces performance while introducing more parameters.

Model	UR-FUNNY ↑	MOSEI ↑	MIMIC ↑	AV-MNIST ↑	Ave ↑
HIGHMMT multitask	63.0	79.9	67.8	70.4	70.3
- w/o embeddings	62.5	78.4	67.9	69.5	69.6
- w/o unimodal	57.6	61.8	63.0	59.1	60.4
- w/o multimodal (Jaegle et al., 2021b; Likhoshesterov et al., 2022)	61.3	80.3	67.7	69.4	69.7
- separate (Tsai et al., 2019; Hendricks et al., 2021)	63.4	79.7	68.5	69.0	70.2
- separate unimodal	64.6	79.9	65.4	69.3	69.9
- separate multimodal	63.5	79.5	65.3	70.0	69.6

MMT results in worse performance. The unimodal encoder is particularly important for best performance. In addition, using separate parameters for unimodal or multimodal layers also decreases performance, which implies that parameter sharing learns improved generalizable representations.

4.7. Understanding information sharing in HIGHMMT

In this subsection, we analyze why this general model achieves strong results in multitask, transfer, and few-shot settings. Based on prior work in multitask learning (Caruana, 1997; Ruder, 2017; Zhang and Yang, 2021), we set up two possible hypotheses: (1) improved generalization and (2) improved regularization. In the former, Caruana (1997) and Ruder (2017) argue that multitask learning improves generalization by leveraging shared information through implicit data augmentation, feature sharing, and common inductive bias across the training signals of related tasks. In this section, we describe several experiments to test the generalization capabilities of HIGHMMT. We investigate the regularization effects of HIGHMMT and include other visualizations and comparisons in Appendix C.4.

Performance under partial-observability. We first evaluate HIGHMMT performance on partially-observable modality subsets during multitask learning (i.e., target task involving modalities not present in the other tasks). From

Table 3, in the large setting, we find that the model performs well on the MIMIC dataset despite its modality set {time-series, table} being completely disjoint from the remaining 3 datasets - we obtain similar performance across both multitask and single-task models (67.8% vs 67.7%). Unsurprisingly, for datasets with more overlap in modality sets (e.g., MOSEI with complete overlap in {text, video, audio}), we find relatively larger improvements using multitask over single-task models (79.9% vs 79.4%). In the medium setting, we find that HIGHMMT multitask also works on ENRICO dataset in the HCI domain (53.1% multitask vs 52.6% single-task) despite it having completely disjoint modality inputs.

Analysis of modality embeddings. From our ablation studies in Table 4, we surprisingly find that removing the modality-specific embedding layer results in only slightly worse performance (70.3 to 69.6 average score). This implies that the shared unimodal encoder has learned generalizable feature extractors that can encode heterogeneous modalities even without a modality identifier.

Parameter sharing. We investigate the extent of parameter sharing in HIGHMMT to measure information sharing across tasks. Using the large setting, we use a gradient-based analysis method (in the same vein of studying gradients to look at prediction influence (Han et al., 2020)) to determine

Table 5. We find evidence of significant **parameter sharing** across unimodal encoders: > 92% of neurons are involved in at least 3 of the 4 tasks. On the other hand, the multimodal layers are more task-specific: only 10% of neurons are involved in 3 or 4 tasks.

HIGHMMT component	Number of involved tasks			
	1	2	3	4
Unimodal encoder	2.8%	5.1%	61.1%	31.1%
Multimodal layer	48.8%	39.7%	9.9%	1.6%

how much each parameter is involved in a specific task. For each task T and parameter $\theta \in \Theta$ in multitask model M_Θ , we compute the involvement $I_T(\theta) = \mathbb{E}_{x,y} |\nabla_\theta M_\Theta(y|x)|$ where $M_\Theta(y|x)$ is the predicted probability of correct target y by M_Θ given x as input. In other words, this measures the absolute gradient with respect to θ when predicting y given x . A higher absolute gradient implies “activated” neurons and vice-versa for gradients closer to 0. This enables us to compute the extent a parameter θ is involved for each task. The *number of tasks* parameter θ is involved in can then be approximated by thresholding and summing up $n(\theta) = \sum_T (\mathbb{1}\{I_T(\theta) > \epsilon \max(I_1(\theta), I_2(\theta), I_3(\theta), I_4(\theta))\})$ which returns an integer from 1 to 4. We chose a threshold ϵ such that parameters are classified as active about half the time on average, which occurs at $\epsilon = 0.2$.

Since we are interested in the level of parameter sharing in the shared unimodal encoder and multimodal layer, we set θ as these 2 modules and report results in Table 5. There is evidence of significant parameter sharing across unimodal encoders: more than 92% of neurons are involved in at least 3 of the 4 tasks. On the other hand, there is not nearly as much parameter sharing in the multimodal layer: only 10% of neurons are involved in 3 or 4 tasks. Hence, the shared unimodal encoders learn task-agnostic representations, but the subsequent multimodal layers (closer to task-specific classifiers) capture more task-specific information.

Negative interference. Another empirical proof for information sharing in multitask models is the phenomenon of catastrophic forgetting (French, 1999; Toneva et al., 2018) - where pre-trained models fine-tuned on a new dataset tend to ‘forget’ how to perform on their pre-trained datasets. We perform a similar experiment of *negative interference*: we pick one task and flip the labels in its training set, train the multitask model on the modified training set, and see how the incorrectly labeled task affects performance on other tasks. This experiment provides evidence of information sharing: if the multitask model does not share information (i.e., the model learns independent subspaces for each task), then one would not observe a negative interference phenomenon from one noisy dataset. We study negative interference under 3 configurations of training (a) the whole model; (b) only the unimodal encoder, and (c) only the multimodal layer.

From Table 6, we observe that certain tasks are more affected by negative interference (e.g., AV-MNIST), while some tasks are not influenced as much (e.g., UR-FUNNY).

Table 6. **Negative interference** shows performance drops on each task (columns) after training on one task with flipped labels (rows). Training the shared unimodal encoders cause the most harm, which implies that unimodal encoders contain more shared neurons sensitive to task changes. **Red** for drops greater than 20%, **yellow** for drops between 10 and 20%, and **green** for drops below 10%.

(a) Training entire model				
Flipped task	UR-FUNNY	MOSEI	MIMIC	AV-MNIST
UR-FUNNY	-24.6	-8.83	-10.6	-57.7
MOSEI	-4.07	-59.7	-20.3	-53.2
MIMIC	-3.59	-5.83	-33.1	-37.5
AV-MNIST	-3.50	-1.23	-4.87	-68.9
(b) Only training unimodal encoder				
Flipped task	UR-FUNNY	MOSEI	MIMIC	AV-MNIST
UR-FUNNY	-23.8	-10.1	-12.8	-58.4
MOSEI	-5.77	-57.6	-21.1	-52.7
MIMIC	-3.03	-3.54	-35.0	-56.3
AV-MNIST	-2.94	-7.82	-53.6	-69.3
(c) Only training multimodal layer				
Flipped task	UR-FUNNY	MOSEI	MIMIC	AV-MNIST
UR-FUNNY	-25.2	-8.34	-2.67	-8.16
MOSEI	0.47	-59.6	-19.8	-8.19
MIMIC	0.19	-0.76	-35.2	-4.87
AV-MNIST	-1.61	-1.48	-2.23	-69.1

This suggests that the nature and degrees of underlying parameter sharing vary across different tasks. Furthermore, we observe that performance drops due to training the shared unimodal encoders are the most significant, which corroborates with our parameter sharing analysis that general unimodal encoders contain more entangled parameters which are more sensitive to task changes. On the other hand, multimodal layers contain more disentangled parameters that share less information across tasks (but are still required for best performance as shown from Table 4 ablation studies).

5. Conclusion

In conclusion, we designed a general model for high-modality and partially-observable scenarios. Our approach:

- (1) Trains multitask models for numerous high-modality and partially-observable multimodal tasks (across 10 modalities, 15 prediction tasks, and 5 research areas), achieving strong performance while reducing total parameters.
- (2) Enables cross-modal information transfer by pretraining on source multimodal tasks before transferring to completely new target modalities and tasks, with larger improvements for low-resource target tasks.
- (3) Improves the tradeoff between performance and efficiency over task-specific state-of-the-art models especially under limited data and partially-observable modalities.
- (4) Reveals surprising insights regarding the nature of information sharing in multimodal and multitask models, which

span generalization and regularization effects.

Finally, we release our code and benchmarks which we hope will present a unified platform for future analysis.

Acknowledgements

This material is based upon work partially supported by the National Science Foundation (Awards #1722822 and #1750439) and National Institutes of Health (Awards #R01MH125740, #R01MH096951, and #U01MH116925). PPL is partially supported by a Facebook PhD Fellowship and a Carnegie Mellon University’s Center for Machine Learning and Health Fellowship. RS is partially supported by NSF IIS1763562 and ONR Grant N000141812861. Any opinions, findings, conclusions, or recommendations expressed in this material are those of the author(s) and do not necessarily reflect the views of the National Science Foundation, National Institutes of Health, Facebook, Carnegie Mellon University’s Center for Machine Learning and Health, or Office of Naval Research, and no official endorsement should be inferred. We are extremely grateful to Aida Nematzadeh, Lisa Anne Hendricks, and students in Louis-Philippe Morency’s and Ruslan Salakhutdinov’s research groups, especially Martin Ma, Chaitanya Ahuja, Volkan Cirik, Peter Wu, Amir Zadeh, Alex Wilf, Victoria Lin, Dong Won Lee, Torsten Wörtwein, and Tiffany Min for helpful discussions and feedback on initial versions of this paper. Finally, we would also like to acknowledge NVIDIA’s GPU support.

References

- Aishwarya Agrawal, Jiasen Lu, Stanislaw Antol, Margaret Mitchell, C. Lawrence Zitnick, Devi Parikh, and Dhruv Batra. VQA: Visual question answering. *International Journal of Computer Vision*, 2017.
- Hassan Akbari, Linagzhe Yuan, Rui Qian, Wei-Hong Chuang, Shih-Fu Chang, Yin Cui, and Boqing Gong. Vatt: Transformers for multimodal self-supervised learning from raw video, audio and text. *arXiv preprint arXiv:2104.11178*, 2021.
- Paras Malik Amisha, Monika Pathania, and Vyas Kumar Rathaur. Overview of artificial intelligence in medicine. *Journal of family medicine and primary care*, 8(7):2328, 2019.
- John Arevalo, Tamar Solorio, Manuel Montes-y Gómez, and Fabio A González. Gated multimodal units for information fusion. In *5th International conference on learning representations 2017 workshop*, 2017.
- Pradeep K Atrey, M Anwar Hossain, Abdulmotaleb El Saddik, and Mohan S Kankanhalli. Multimodal fusion for multimedia analysis: a survey. *Multimedia systems*, 16(6):345–379, 2010.
- Tadas Baltrušaitis, Chaitanya Ahuja, and Louis-Philippe Morency. Multimodal machine learning: A survey and taxonomy. *IEEE transactions on pattern analysis and machine intelligence*, 41(2):423–443, 2018.
- Jonathan Baxter. A bayesian/information theoretic model of learning to learn via multiple task sampling. *Machine learning*, 28(1):7–39, 1997.
- Tony Belpaeme, James Kennedy, Aditi Ramachandran, Brian Scassellati, and Fumihide Tanaka. Social robots for education: A review. *Science robotics*, 3(21), 2018.
- Rich Caruana. Multitask learning. *Machine learning*, 28(1):41–75, 1997.
- Devendra Singh Chaplot, Kanthashree Mysore Sathyendra, Rama Kumar Pasumarthi, Dheeraj Rajagopal, and Ruslan Salakhutdinov. Gated-attention architectures for task-oriented language grounding. In *Thirty-Second AAAI Conference on Artificial Intelligence*, 2018.
- Yen-Chun Chen, Linjie Li, Licheng Yu, Ahmed El Kholy, Faisal Ahmed, Zhe Gan, Yu Cheng, and Jingjing Liu. Uniter: Universal image-text representation learning. In *European conference on computer vision*, pages 104–120. Springer, 2020.
- Jaemin Cho, Jie Lei, Hao Tan, and Mohit Bansal. Unifying vision-and-language tasks via text generation. In *ICML*, 2021.
- Biplab Deka, Zifeng Huang, Chad Franzen, Joshua Hibsichman, Daniel Afergan, Yang Li, Jeffrey Nichols, and Ranjitha Kumar. Rico: A mobile app dataset for building data-driven design applications. In *Proceedings of the 30th Annual ACM Symposium on User Interface Software and Technology*, pages 845–854, 2017.
- Jacob Devlin, Ming-Wei Chang, Kenton Lee, and Kristina Toutanova. Bert: Pre-training of deep bidirectional transformers for language understanding. In *NAACL-HLT (1)*, 2019.
- Alan Dix, Janet Finlay, Gregory D Abowd, and Russell Beale. Human-computer interaction. *Harlow ua*, 2000.
- Alexey Dosovitskiy, Lucas Beyer, Alexander Kolesnikov, Dirk Weissenborn, Xiaohua Zhai, Thomas Unterthiner, Mostafa Dehghani, Matthias Minderer, Georg Heigold, Sylvain Gelly, et al. An image is worth 16x16 words: Transformers for image recognition at scale. *ICLR*, 2021.
- Jared Dunnmon, Alexander Ratner, Nishith Khandwala, Khaled Saab, Matthew Markert, Hersh Sagreiya, Roger E. Goldman, Christopher Lee-Messer, Matthew P. Lungren, Daniel L. Rubin, and Christopher Ré. Cross-modal data programming enables rapid medical machine learning. *CoRR*, abs/1903.11101, 2019. URL <http://arxiv.org/abs/1903.11101>.
- Robert M French. Catastrophic forgetting in connectionist networks. *Trends in cognitive sciences*, 3(4):128–135, 1999.
- Pascal Hamisu, Gregor Heinrich, Christoph Jung, Volker Hahn, Carlos Duarte, Pat Langdon, and Pradipta Biswas. Accessible ui design and multimodal interaction through hybrid tv platforms: towards a virtual-user centered design framework. In *International Conference on Universal Access in Human-Computer Interaction*, pages 32–41. Springer, 2011.
- Xiaochuang Han, Byron C Wallace, and Yulia Tsvetkov. Explaining black box predictions and unveiling data artifacts through influence functions. In *Proceedings of the 58th Annual Meeting of the Association for Computational Linguistics*, pages 5553–5563, 2020.

- Md Kamrul Hasan, Wasifur Rahman, AmirAli Bagher Zadeh, Jianyuan Zhong, Md Iftekhar Tanveer, Louis-Philippe Morency, and Mohammed Ehsan Hoque. Ur-funny: A multimodal language dataset for understanding humor. In *Proceedings of the 2019 Conference on Empirical Methods in Natural Language Processing and the 9th International Joint Conference on Natural Language Processing (EMNLP-IJCNLP)*, pages 2046–2056, 2019.
- Lisa Anne Hendricks, John Mellor, Rosalia Schneider, Jean-Baptiste Alayrac, and Aida Nematzadeh. Decoupling the role of data, attention, and losses in multimodal transformers. *arXiv preprint arXiv:2102.00529*, 2021.
- Ronghang Hu and Amanpreet Singh. Transformer is all you need: Multimodal multitask learning with a unified transformer. *arXiv preprint arXiv:2102.10772*, 2021.
- Andrew Jaegle, Sebastian Borgeaud, Jean-Baptiste Alayrac, Carl Doersch, Catalin Ionescu, David Ding, Skanda Koppula, Daniel Zoran, Andrew Brock, Evan Shelhamer, et al. Perceiver io: A general architecture for structured inputs & outputs. *arXiv preprint arXiv:2107.14795*, 2021a.
- Andrew Jaegle, Felix Gimeno, Andrew Brock, Andrew Zisserman, Oriol Vinyals, and Joao Carreira. Perceiver: General perception with iterative attention. *arXiv preprint arXiv:2103.03206*, 2021b.
- Siddhant M. Jayakumar, Wojciech M. Czarnecki, Jacob Menick, Jonathan Schwarz, Jack Rae, Simon Osindero, Yee Whye Teh, Tim Harley, and Razvan Pascanu. Multiplicative interactions and where to find them. In *International Conference on Learning Representations*, 2020. URL <https://openreview.net/forum?id=rylnK6VtDH>.
- Alistair EW Johnson, Tom J Pollard, Lu Shen, H Lehman Li-Wei, Mengling Feng, Mohammad Ghassemi, Benjamin Moody, Peter Szolovits, Leo Anthony Celi, and Roger G Mark. Mimic-iii, a freely accessible critical care database. *Scientific data*, 3(1): 1–9, 2016.
- Lukasz Kaiser, Aidan N Gomez, Noam Shazeer, Ashish Vaswani, Niki Parmar, Llion Jones, and Jakob Uszkoreit. One model to learn them all. *arXiv preprint arXiv:1706.05137*, 2017.
- Will Kay, Joao Carreira, Karen Simonyan, Brian Zhang, Chloe Hillier, Sudheendra Vijayanarasimhan, Fabio Viola, Tim Green, Trevor Back, Paul Natsev, et al. The kinetics human action video dataset. *arXiv preprint arXiv:1705.06950*, 2017.
- Sahar Kazemzadeh, Vicente Ordonez, Mark Matten, and Tamara Berg. Referitgame: Referring to objects in photographs of natural scenes. In *Proceedings of the 2014 conference on empirical methods in natural language processing (EMNLP)*, pages 787–798, 2014.
- Douwe Kiela, Suvrat Bhooshan, Hamed Firooz, Ethan Perez, and Davide Testuggine. Supervised multimodal bitransformers for classifying images and text. *arXiv preprint arXiv:1909.02950*, 2019.
- Douwe Kiela, Hamed Firooz, Aravind Mohan, Vedanuj Goswami, Amanpreet Singh, Pratik Ringshia, and Davide Testuggine. The hateful memes challenge: Detecting hate speech in multimodal memes. *Advances in Neural Information Processing Systems*, 33, 2020.
- Elizabeth S Kim, Lauren D Berkovits, Emily P Bernier, Dan Leyzberg, Frederick Shic, Rhea Paul, and Brian Scassellati. Social robots as embedded reinforcers of social behavior in children with autism. *Journal of autism and developmental disorders*, 43(5):1038–1049, 2013.
- Elsa A Kirchner, Stephen H Fairclough, and Frank Kirchner. Embedded multimodal interfaces in robotics: applications, future trends, and societal implications. In *The Handbook of Multimodal-Multisensor Interfaces: Language Processing, Software, Commercialization, and Emerging Directions-Volume 3*, pages 523–576. 2019.
- Alex Krizhevsky, Geoffrey Hinton, et al. Learning multiple layers of features from tiny images. 2009.
- Yann LeCun, Léon Bottou, Yoshua Bengio, and Patrick Haffner. Gradient-based learning applied to document recognition. *Proceedings of the IEEE*, 86(11):2278–2324, 1998.
- Per Ledin and David Machin. *Introduction to multimodal analysis*. Bloomsbury Publishing, 2020.
- Michelle A Lee, Yuke Zhu, Krishnan Srinivasan, Parth Shah, Silvio Savarese, Li Fei-Fei, Animesh Garg, and Jeannette Bohg. Making sense of vision and touch: Self-supervised learning of multimodal representations for contact-rich tasks. In *2019 International Conference on Robotics and Automation (ICRA)*, pages 8943–8950. IEEE, 2019.
- Michelle A Lee, Brent Yi, Roberto Martín-Martín, Silvio Savarese, and Jeannette Bohg. Multimodal sensor fusion with differentiable filters. *IROS*, 2020a.
- Michelle A Lee, Yuke Zhu, Peter Zachares, Matthew Tan, Krishnan Srinivasan, Silvio Savarese, Li Fei-Fei, Animesh Garg, and Jeannette Bohg. Making sense of vision and touch: Learning multimodal representations for contact-rich tasks. *IEEE Transactions on Robotics*, 36(3):582–596, 2020b.
- Sangho Lee, Youngjae Yu, Gunhee Kim, Thomas Breuel, Jan Kautz, and Yale Song. Parameter efficient multimodal transformers for video representation learning. In *International Conference on Learning Representations*, 2020c.
- Luis A Leiva, Asutosh Hota, and Antti Oulasvirta. Enrico: A dataset for topic modeling of mobile ui designs. In *22nd International Conference on Human-Computer Interaction with Mobile Devices and Services (MobileHCI'20 Extended Abstracts)*, 2020.
- R Gary Leonard and George Doddington. Tidigits speech corpus. *Texas Instruments, Inc*, 1993.
- Liunian Harold Li, Mark Yatskar, Da Yin, Cho-Jui Hsieh, and Kai-Wei Chang. Visualbert: A simple and performant baseline for vision and language. *arXiv preprint arXiv:1908.03557*, 2019.
- Qing Li, Boqing Gong, Yin Cui, Dan Kondratyuk, Xianzhi Du, Ming-Hsuan Yang, and Matthew Brown. Towards a unified foundation model: Jointly pre-training transformers on unpaired images and text. *arXiv preprint arXiv:2112.07074*, 2021.
- Yaoyiran Li, Edoardo Maria Ponti, Ivan Vulić, and Anna Korhonen. Emergent communication pretraining for few-shot machine translation. In *Proceedings of the 28th International Conference on Computational Linguistics*, pages 4716–4731, 2020.

- Paul Pu Liang, Zhun Liu, Yao-Hung Hubert Tsai, Qibin Zhao, Ruslan Salakhutdinov, and Louis-Philippe Morency. Learning representations from imperfect time series data via tensor rank regularization. In *ACL*, 2019.
- Paul Pu Liang, Terrance Liu, Anna Cai, Michal Muszynski, Ryo Ishii, Nicholas Allen, Randy Auerbach, David Brent, Ruslan Salakhutdinov, and Louis-Philippe Morency. Learning language and multimodal privacy-preserving markers of mood from mobile data. In *ACL/IJCNLP (1)*, 2021a.
- Paul Pu Liang, Yiwei Lyu, Xiang Fan, Zetian Wu, Yun Cheng, Jason Wu, Leslie Yufan Chen, Peter Wu, Michelle A Lee, Yuke Zhu, et al. Multibench: Multiscale benchmarks for multimodal representation learning. In *NeurIPS Datasets and Benchmarks Track*, 2021b.
- Paul Pu Liang, Peter Wu, Liu Ziyin, Louis-Philippe Morency, and Ruslan Salakhutdinov. Cross-modal generalization: Learning in low resource modalities via meta-alignment. In *Proceedings of the 29th ACM International Conference on Multimedia*, pages 2680–2689, 2021c.
- Valerii Likhoshesterov, Mostafa Dehghani, Anurag Arnab, Krzysztof Marcin Choromanski, Mario Lucic, Yi Tay, and Adrian Weller. Polyvit: Co-training vision transformers on images, videos and audio, 2022. URL https://openreview.net/forum?id=9r4_7GxTLnS.
- Bryan Lim, Serkan Ö Arik, Nicolas Loeff, and Tomas Pfister. Temporal fusion transformers for interpretable multi-horizon time series forecasting. *International Journal of Forecasting*, 2021.
- Jiasen Lu, Dhruv Batra, Devi Parikh, and Stefan Lee. Vilmert: pre-training task-agnostic visiolinguistic representations for vision-and-language tasks. In *Proceedings of the 33rd International Conference on Neural Information Processing Systems*, pages 13–23, 2019.
- Kevin Lu, Aditya Grover, Pieter Abbeel, and Igor Mordatch. Pre-trained transformers as universal computation engines. *arXiv preprint arXiv:2103.05247*, 2021.
- George A. Miller. Wordnet: A lexical database for english. *Commun. ACM*, 38(11):39–41, November 1995. ISSN 0001-0782.
- Jiquan Ngiam, Aditya Khosla, Mingyu Kim, Juhan Nam, Honglak Lee, and Andrew Y Ng. Multimodal deep learning. In *ICML*, 2011.
- Isabel Papadimitriou and Dan Jurafsky. Learning music helps you read: Using transfer to study linguistic structure in language models. In *Proceedings of the 2020 Conference on Empirical Methods in Natural Language Processing (EMNLP)*, pages 6829–6839, 2020.
- Ethan Perez, Florian Strub, Harm de Vries, Vincent Dumoulin, and Aaron C Courville. Film: Visual reasoning with a general conditioning layer. In *AAAI*, 2018.
- Rosalind W Picard. *Affective computing*. MIT press, 2000.
- Karol J Piczak. Esc: Dataset for environmental sound classification. In *Proceedings of the 23rd ACM international conference on Multimedia*, pages 1015–1018, 2015.
- Bryan A Plummer, Liwei Wang, Chris M Cervantes, Juan C Caicedo, Julia Hockenmaier, and Svetlana Lazebnik. Flickr30k entities: Collecting region-to-phrase correspondences for richer image-to-sentence models. In *Proceedings of the IEEE international conference on computer vision*, pages 2641–2649, 2015.
- Soujanya Poria, Erik Cambria, Rajiv Bajpai, and Amir Hussain. A review of affective computing: From unimodal analysis to multimodal fusion. *Information Fusion*, 2017.
- Aditya Ramesh, Mikhail Pavlov, Gabriel Goh, Scott Gray, Chelsea Voss, Alec Radford, Mark Chen, and Ilya Sutskever. Zero-shot text-to-image generation. *arXiv preprint arXiv:2102.12092*, 2021.
- Sebastian Ruder. An overview of multi-task learning in deep neural networks. *arXiv preprint arXiv:1706.05098*, 2017.
- Rajiv Shah and Roger Zimmermann. *Multimodal analysis of user-generated multimedia content*. Springer, 2017.
- Amanpreet Singh, Ronghang Hu, Vedanuj Goswami, Guillaume Couairon, Wojciech Galuba, Marcus Rohrbach, and Douwe Kiela. Flava: A foundational language and vision alignment model. *arXiv preprint arXiv:2112.04482*, 2021.
- Richard Socher, Milind Ganjoo, Hamsa Sridhar, Osbert Bastani, Christopher D Manning, and Andrew Y Ng. Zero-shot learning through cross-modal transfer. *arXiv preprint arXiv:1301.3666*, 2013.
- Weijie Su, Xizhou Zhu, Yue Cao, Bin Li, Lewei Lu, Furu Wei, and Jifeng Dai. Vi-bert: Pre-training of generic visual-linguistic representations. In *International Conference on Learning Representations*, 2020. URL <https://openreview.net/forum?id=SygXPaEYvH>.
- Chen Sun, Austin Myers, Carl Vondrick, Kevin Murphy, and Cordelia Schmid. Videobert: A joint model for video and language representation learning. In *Proceedings of the IEEE/CVF International Conference on Computer Vision*, pages 7464–7473, 2019.
- Hao Tan and Mohit Bansal. Lxmert: Learning cross-modality encoder representations from transformers. In *Proceedings of the 2019 Conference on Empirical Methods in Natural Language Processing and the 9th International Joint Conference on Natural Language Processing (EMNLP-IJCNLP)*, pages 5100–5111, 2019.
- Mariya Toneva, Alessandro Sordoni, Remi Tachet des Combes, Adam Trischler, Yoshua Bengio, and Geoffrey J Gordon. An empirical study of example forgetting during deep neural network learning. In *International Conference on Learning Representations*, 2018.
- Yao-Hung Hubert Tsai, Shaojie Bai, Paul Pu Liang, J Zico Kolter, Louis-Philippe Morency, and Ruslan Salakhutdinov. Multimodal transformer for unaligned multimodal language sequences. In *Proceedings of the 57th Annual Meeting of the Association for Computational Linguistics*, pages 6558–6569, 2019.
- Ashish Vaswani, Noam Shazeer, Niki Parmar, Jakob Uszkoreit, Llion Jones, Aidan N Gomez, Lukasz Kaiser, and Illia Polosukhin. Attention is all you need. In *NIPS*, 2017.

- Valentin Vielzeuf, Alexis Lechervy, Stéphane Pateux, and Frédéric Jurie. Centralnet: a multilayer approach for multimodal fusion, 2018.
- Weiyao Wang, Du Tran, and Matt Feiszli. What makes training multi-modal classification networks hard? In *Proceedings of the IEEE/CVF Conference on Computer Vision and Pattern Recognition*, pages 12695–12705, 2020.
- Yuhuai Wu, Markus N. Rabe, Wenda Li, Jimmy Ba, Roger B. Grosse, and Christian Szegedy. LIME: learning inductive bias for primitives of mathematical reasoning. In Marina Meila and Tong Zhang, editors, *Proceedings of the 38th International Conference on Machine Learning, ICML 2021, 18-24 July 2021, Virtual Event*, volume 139 of *Proceedings of Machine Learning Research*, pages 11251–11262. PMLR, 2021. URL <http://proceedings.mlr.press/v139/wu21c.html>.
- Chen Xing, Negar Rostamzadeh, Boris Oreshkin, and Pedro O. O. Pinheiro. Adaptive cross-modal few-shot learning. In H. Wallach, H. Larochelle, A. Beygelzimer, F. d'Alché-Buc, E. Fox, and R. Garnett, editors, *Advances in Neural Information Processing Systems 32*. 2019. URL <http://papers.nips.cc/paper/8731-adaptive-cross-modal-few-shot-learning.pdf>.
- Shaowei Yao and Xiaojun Wan. Multimodal transformer for multimodal machine translation. In *Proceedings of the 58th Annual Meeting of the Association for Computational Linguistics*, Online, July 2020. Association for Computational Linguistics. doi: 10.18653/v1/2020.acl-main.400. URL <https://www.aclweb.org/anthology/2020.acl-main.400>.
- De Jong Yeong, Gustavo Velasco-Hernandez, John Barry, Joseph Walsh, et al. Sensor and sensor fusion technology in autonomous vehicles: A review. *Sensors*, 21(6):2140, 2021.
- Peter Young, Alice Lai, Micah Hodosh, and Julia Hockenmaier. From image descriptions to visual denotations: New similarity metrics for semantic inference over event descriptions. *Transactions of the Association for Computational Linguistics*, 2:67–78, 2014. doi: 10.1162/tacl.a.00166. URL <https://aclanthology.org/Q14-1006>.
- Amir Zadeh, Paul Pu Liang, and Louis-Philippe Morency. Foundations of multimodal co-learning. *Information Fusion*, 64: 188–193, 2020.
- AmirAli Bagher Zadeh, Paul Pu Liang, Soujanya Poria, Erik Cambria, and Louis-Philippe Morency. Multimodal language analysis in the wild: Cmu-mosei dataset and interpretable dynamic fusion graph. In *ACL*, 2018.
- Rowan Zellers, Yonatan Bisk, Ali Farhadi, and Yejin Choi. From recognition to cognition: Visual commonsense reasoning. In *Proceedings of the IEEE/CVF Conference on Computer Vision and Pattern Recognition*, pages 6720–6731, 2019.
- Yu Zhang and Qiang Yang. A survey on multi-task learning. *IEEE Transactions on Knowledge and Data Engineering*, 2021.

Appendix

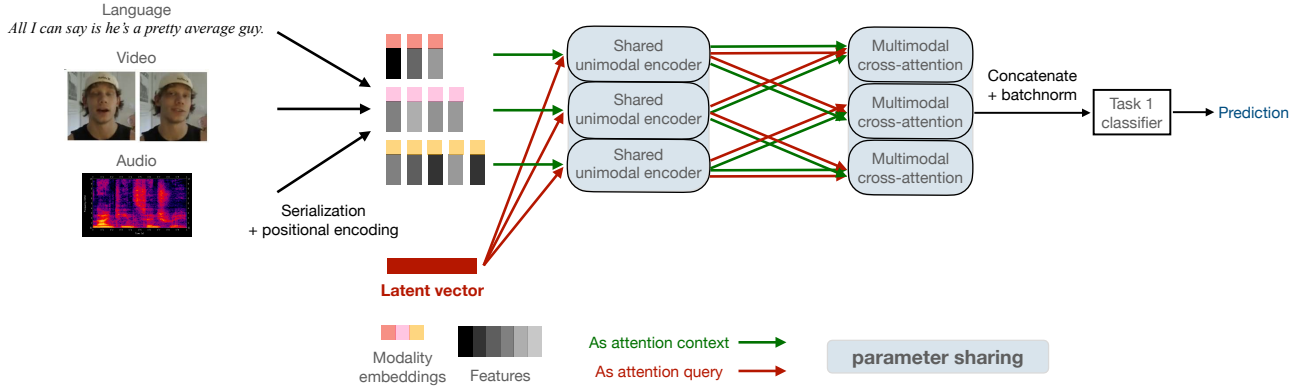


Figure 6. General architecture of HIGHMMT: Given arbitrary modalities, (1) the inputs are standardized into a sequence and padded, (2) modality embeddings and positional encodings are added to the serialized raw input, (3) a single shared unimodal Perceiver encoder is applied to all modalities to learn general-purpose representations regardless of the specific input modality, (4) each pair of unimodal representations is fed through a shared multimodal cross-attention layer twice (the first time with one modality as query and the other as context, and the second time vice versa) to learn general multimodal representations regardless of the input modalities and task, and finally (5) all outputs from cross-attention layers are concatenated, batch-normalized, and fed through a task-specific classification head to make a prediction. The unimodal encoders and multimodal layers are shared across tasks during multitask learning to enable statistical strength sharing, parameter efficiency, and quick generalization across diverse modalities and tasks.

A. Model Implementation Details

At a high level, HIGHMMT includes the following components: (1) the inputs are standardized into a sequence and padded, (2) the perceiver input processing adds modality-specific modality embeddings and positional encodings to the serialized raw input; (3) the processed input from each modality is fed into a shared unimodal perceiver encoder; (4) each pair of unimodal perceiver output (unimodal representations) is fed through a shared crossmodal transformer layer twice (the first time with one modality as query and the other as context, and the second time vice versa); (5) finally, all outputs from multimodal layers are concatenated, batch-normalized to form a multimodal representation, and fed through a task-specific classification head to make a prediction. Figure 6 is an illustration of the high-level architecture.

A.1. Perceiver Input Processing

We follow the data processing pipeline in the GitHub implementation for multimodal perceivers: <https://github.com/fac2003/perceiver-multi-modality-pytorch>. For each modality, we must specify in advance the channel size (i.e., embedding size) and how many extra dimensions there are other than the channel/embedding dimension.

The modality embedding is just a one-hot vector denoting the index of the current modality, and the size of the vector is equal to the total number of modalities involved. This embedding layer identifies common modalities across different tasks to enable sharing of information. For example, the modality embedding of the image sequence for a video classification task will be shared with that of an input (static) image for an image and text question-answering task.

We also specify a few hyperparameters (such as `num_freq_bands` and `max_freq`) for the Fourier transformation used in the positional encoding. The positional encoding represents where this embedding is at through Fourier transformations (so if there is 1 extra dimension, then the positional encoding will encode the 1D position of each embedding; if there are 2 extra dimensions, then the positional encoding will encode the 2D position of each embedding). The positional encoding length can vary for each modality depending on the number of extra dimensions and the Fourier transformation hyperparameters.

The total embedding size of the processed output will be equal to $d_{all} = \max_{m \in M} (d_m + d_{pm} + |M|)$, where M is the set of all modalities involved, d_m is the channel size of modality m , d_{pm} is the positional encoding size of modality m , and $|M|$ is the modality encoding size (i.e., the total number of involved modalities). When processing each modality, we concatenate the input channels, the positional encoding, and the modality encoding along the channel/embedding axis before adding

zero-padding along this axis to match a desired total embedding size d_{all} . As a result, all modalities will be processed to have the same embedding size d_{all} . We also flatten all non-embedding dimensions so the processed input will always have shape $n \times t_m \times d_{all}$ where n is a common batchsize, t_m is a modality-specific sequence length, and d_{all} is the common embedding dimension.

For example, during multitask learning in the large setting (4 datasets involved: UR-FUNNY, MOSEI, MIMIC, and AV-MNIST), $d_{all} = 387$ (because the image modality from UR-FUNNY has a channel size of 371, positional encoding size of 7, and modality encoding size of 9). When processing the colorless image modality from AVMNIST ($7 \times 7 \times 16$), we have a channel size of 16, positional encoding size of 26, and modality encoding size of 9, so the processed output will be 49×387 where the first 16 dimensions along the last dimension represent 16 raw input dimensions, the next 336 dimensions are padded zeroes, the next 26 dimensions are positional encodings, and the final 9 dimensions are modality encodings.

Note that during this entire processing step all procedures are programmatic and there are no trainable parameters involved.

A.2. Unimodal Perceiver Encoder

Now that we have standardized all modality inputs into a common representation, we follow the Perceiver architecture (Jaegle et al., 2021b) to perform modality and task-agnostic representation learning from each input modality. Starting with a latent array of shape $d_{LN} \times d_{LS}$ (array size configurable as a hyperparameter, where d_{LN} is the number of latent vectors and d_{LS} is the latent dimension) with trainable initialization, for each layer, we first perform cross-attention on the latent array using the processed input array (of shape $t_m \times d_{all}$) as context. Cross-attention between the latent vector and the input modality sequence learns relationships between elements in each modality, resulting in unimodal contextualized representations. The resulting latent array then goes through a latent transformer (with self-attention and feed-forward layers). We repeat this architecture for each layer within the encoder. The main advantage of this Perceiver encoder is that it can encode the input into a common $d_{LN} \times d_{LS}$ latent array regardless of the input shape $t_m \times d_{all}$, and the total runtime is linear with respect to the size of t_m which scales to high-modality scenarios. Note that only one copy of a unimodal Transformer (Perceiver) block is used to encode all modalities simultaneously, which enables statistical strength sharing and general-purpose representation learning regardless of the specific input modality.

A.3. Crossmodal Transformer layer

To learn modality and task-agnostic multimodal representations, we use multiple layers of a general-purpose Crossmodal Transformer block (Tsai et al., 2019; Lu et al., 2019). Given 2 unimodal representations \mathbf{z}_1 and \mathbf{z}_2 of common shape $d_{LN} \times d_{LS}$ learned from unimodal Perceiver encoders, a Crossmodal Transformer (CT) block uses crossmodal self-attention by setting the input layer query $Q = \mathbf{z}_1$ and keys and values $K, V = \mathbf{z}_2$ to learn attention from modality 1 to modality 2, and a separate block to capture the attention in the opposite direction. This step enables one modality’s sequence elements to discover correspondences in another. A Crossmodal Transformer block using \mathbf{z}_1 to attend to \mathbf{z}_2 (and vice-versa) results in a multimodal representation $\mathbf{z}_{mm} = [\mathbf{z}_{1 \rightarrow 2}, \mathbf{z}_{2 \rightarrow 1}] = [\text{CT}(\mathbf{z}_1, \mathbf{z}_2), \text{CT}(\mathbf{z}_2, \mathbf{z}_1)]$. For each layer, we first perform cross-attention followed by self-attention and feed-forward functions. In the end, we only take the last d_{LS} -dimensional vector out of the $d_{LN} \times d_{LS}$ final latent array as the output of this module. For tasks with more than 2 modalities, a Crossmodal Transformer block is applied for each pair of modalities before concatenating all multimodal representations. Again, only one copy of a multimodal layer is used on all tasks to learn general representations regardless of the input modalities and task.

A.4. Task-specific classifiers

Since each task may have a different number of modalities and output classes, we create a separate classification head for each task. For each classification head, it concatenates all outputs of the Crossmodal Transformer layer (so 2-modality tasks have concatenated size of $2d_{LS}$, 3-modality tasks have concatenated size of $6d_{LS}$, etc), performs batch-normalization, and feeds the normalized multimodal representation \mathbf{z}_{mm} into a linear layer that maps to the logits for this task. This classification layer composes individual correspondences learned within and across modalities to form a final prediction.

A.5. Multitask training details

Since each task has a different number of training batches, not all tasks will be involved in each training step. We arrange the tasks to be included in each training step such that more tasks will be trained simultaneously towards the end of an epoch. For example, if task A has 300 training batches, task B has 200 training batches, and task C has 100 training batches, then

for the first 100 training steps in an epoch, only task A will be used; then for the next 100 steps both A and B will be used; and for the last 100 steps, all three tasks will be used. This approach tends to work better than including all tasks in all steps via uniform batch sampling because the task with fewer training batches tends to overfit in the latter approach.

Within each training step, we compute the losses of the batch from each task used and compute the gradient using a weighted sum of the losses. The weights are part of the hyperparameters that we can tune to ensure balanced training. Then we update the model using the computed gradients.

We compute validation performance after each epoch for each task, and aggregate validation performances across all tasks (this is necessary because different tasks are measured differently, sometimes bigger is better, sometimes smaller is better). When all tasks are accuracy-based (such as the large setting), we just weigh them equally. Then we report test performance on the checkpoint with the highest aggregated validation performance.

A.6. Transfer learning details

If we are trying to transfer from tasks $\{A, B, C\}$ to D , initially we start with a randomly initialized HIGHMMT model that defines modality embeddings for all modalities in $\{A, B, C, D\}$ as well as a classification head for each. Then, we pretrain the model using multitask learning on $\{A, B, C\}$ using the same procedure as before. After saving a good checkpoint as measured by aggregated validation performance on pretraining tasks $\{A, B, C\}$, we finetune the trained model on target task D . The modality and tasks in $\{A, B, C\}$ present during multitask pretraining can be very different from those encountered in D during fine-tuning.

A.7. Few-shot multitask learning details

In section 4.4, we also investigated few-shot learning using limited labeled data in a target task. When we perform few-shot learning on task D with the help of tasks $\{A, B, C\}$, we jointly train $\{A, B, C, D\}$ together in the same multitask manner as before, but since we don't care about the performance of our model on auxiliary tasks $\{A, B, C\}$, we assign a higher weight to the losses on task D and keep track of the best validation performance on D when selecting checkpoints.

B. Experimental Setup

In this section, we provide additional details on the experimental setup to analyze the multitask, transfer, and generalization capabilities of HIGHMMT.

B.1. Setup

We use a large collection of multimodal datasets provided in the standardized and public MultiBench benchmark (Liang et al., 2021b). This benchmark spans 15 real-world datasets, 10 modalities, 20 prediction tasks, and 6 research areas. Each of these datasets requires a model to learn basic representations of features in each modality and aggregate complementary information across multiple modalities to make a prediction.

Affective computing involves understanding our natural display of multimodal signals spanning language (spoken words), visual (facial expressions, gestures), and acoustic (prosody, speech tone) in order to predict human affective states (emotions, sentiment, and personalities) (Picard, 2000). We test on 2 datasets involving fusing *language*, *video*, and *audio* time-series data to predict sentiment and emotions (MOSEI (Zadeh et al., 2018)) as well as humor (UR-FUNNY (Hasan et al., 2019)).

Healthcare: Medical decision-making often involves integrating multiple sensory readings from instruments such as lab tests, imaging reports, and patient-doctor conversations (Amisha et al., 2019). We experiment with the large-scale MIMIC dataset (Johnson et al., 2016) which records ICU patient data including *time-series* data measured every hour and other demographic variables in the form of *tabular numerical* data. These are used to predict the disease ICD-9 code and mortality rate.

Robotics: Modern robot systems are equipped with multiple sensors in order to capture complementary signals useful for holistic decision-making. We test on the large-scale MuJoCo PUSH (Lee et al., 2020a) and V&T (Vision&Touch) (Lee et al., 2020b) datasets which record the manipulation of simulated and real robotic arms equipped with *visual* (RGB and depth), *force*, and *proprioception* sensors. In PUSH, the goal is to predict the pose of the object being pushed by the robot end-effector. In V&T, the goal is to predict action-conditional learning objectives that capture forward dynamics (contact prediction and robot end-effector pose).

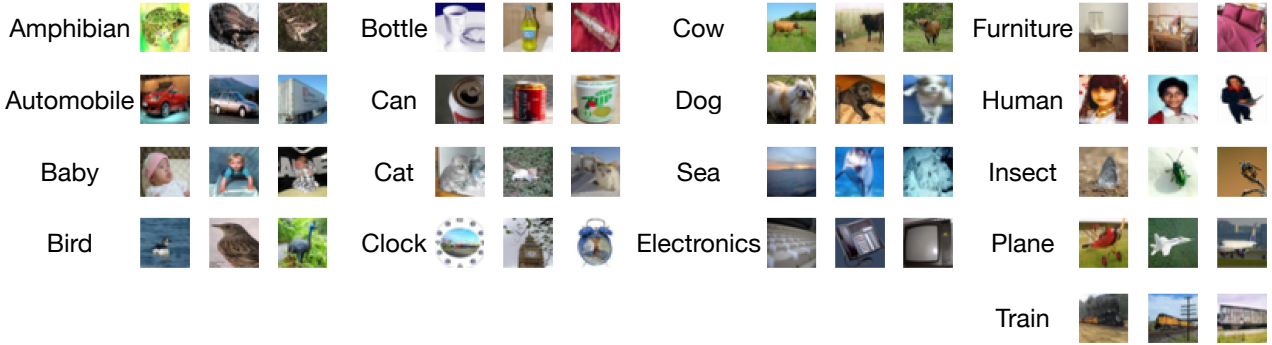


Figure 7. The 17 concepts shared across image and audio datasets that were used to define positive retrieval groups in CIFAR-ESC. Note that we only show the images - the audio spectrograms make up the second modality in each concept.

Table 7. We investigate 3 multitask training setups to evaluate the performance of HIGHMMT. Each multitask setup is designed to include tasks with different modality inputs and prediction objectives. The total size of datasets involved in our experiments exceeds 370,000 and covers diverse modalities such as time-series, various robotics sensors, sets, and tables, as well as multiple research areas and prediction tasks from affective computing, healthcare, multimedia, robotics, and HCI.

Setting	Datasets	Modalities	Size	Prediction task	Research Area
Small	PUSH	{image, force, proprioception, control}	37,990	object pose	Robotics
	V&T	{image, force, proprioception, depth}	147,000	contact, robot pose	Robotics
Medium	ENRICO	{image, set}	1,460	design interface	HCI
	PUSH AV-MNIST	{image, force, proprioception, control} {image, audio}	37,990 70,000	object pose digit	Robotics Multimedia
Large	UR-FUNNY	{text, video, audio}	16,514	humor	Affective Computing
	MOSEI	{text, video, audio}	22,777	sentiment, emotions	Affective Computing
	MIMIC	{time-series, table}	36,212	mortality, ICD-9 codes	Healthcare
	AV-MNIST	{image, audio}	70,000	digit	Multimedia

Human Computer Interaction (HCI) studies the design of computer technology and interactive interfaces between humans and computers (Dix et al., 2000). We use the ENRICO dataset (Deka et al., 2017; Leiva et al., 2020) of Android app screens (consisting of an *image* as well as a *set* of apps and their locations) categorized by their design motifs and collected for data-driven design applications such as design search, user interface (UI) layout generation, UI code generation, and user interaction modeling.

Multimedia: A significant body of research in multimodal learning has been fueled by the large availability of multimedia data (language, image, video, and audio) on the internet. We experiment on 2 large-scale multimedia datasets with varying sizes and levels of difficulty: (1) AV-MNIST (Vielzeuf et al., 2018) is assembled from *images* of handwritten digits (LeCun et al., 1998) and *audio* samples of spoken digits (Leonard and Doddington, 1993), and (2) CIFAR-ESC (Liang et al., 2021c) is an image-audio retrieval dataset. To construct CIFAR-ESC, we follow Liang et al. (2021c) and combine 100 classes from CIFAR-100 and 10 classes from CIFAR-10 (Krizhevsky et al., 2009) to form 110 image classes, as well as 50 audio classes from ESC-50 (Piczak, 2015). To bridge these two modalities with partially related label spaces, we define 17 shared classes across the 2 datasets for weak concept alignment. These clusters are obtained by mapping similar classes between the datasets using similarities from WordNet (Miller, 1995) and text cooccurrence, and we show the resulting 17 clustered concepts we used for weak alignment in Figure 7. For the retrieval task, we first split all images and audio into a 3/1/1 train/valid/test split. Within each split, we paired each image with one randomly selected audio clip from the same shared class and label that pair as positive, and with one randomly selected audio clip from a different shared class and label that pair as negative. We evaluate retrieval performance via binary classification accuracy of an image and audio clip classified into either positive or negative pairs. The final retrieval dataset consists of 38K training pairs, 13K validation pairs and 13K test pairs.

Multitask setup: We trained 3 multitask models across combinations of the aforementioned datasets. Each multitask setup is designed to include tasks with different modality inputs and prediction objectives.

1. **Small:** PUSH, V&T: 2 tasks in the same research area (robotics) but with different modality inputs: {image, force, proprioception, control} and {image, force, proprioception, depth} respectively. Furthermore, each robot’s

sensor readings come from different robot-dependent sensors.

2. **Medium:** ENRICO, PUSH, AV-MNIST across 3 domains (multimedia, HCI, and robotics) with different modalities: {image, set}, {image, force, proprioception, control}, and {image, audio}.

3. **Large:** UR-FUNNY, MOSEI, MIMIC, and AV-MNIST, across 3 domains (affective computing, healthcare, and multimedia), again with different modalities: {text, video, audio} for the first 2 tasks with different format of preprocessed embeddings of video and audio, {time-series, table}, and {image, audio}.

We summarize these experimental settings in Table 7. Overall, the total size of datasets involved in our experiments exceeds 370,000 and covers diverse modalities such as time-series, various robotics sensors, sets, and tables, as well as multiple research areas and prediction tasks from affective computing, healthcare, multimedia, robotics, and HCI.

B.2. Hyperparameters and training details

We list hyperparameters used throughout our models in Table 8, Table 9, and Table 10 for small, medium, and large multitask settings respectively. Code is also included in the supplementary material for reproducibility.

Table 8. Table of hyperparameters for multitask prediction on the **small** setting involving PUSH, V&T: 2 tasks in the same research area (robotics) but with different modality inputs: {image, force, proprioception, control} and {image, force, proprioception, depth} respectively, and readings come from different robot-dependent sensors.

Part of Model	Hyperparameter	Values	
		PUSH	V&T
Unimodal Perceiver Encoder	Depth	1	
	Num Latents	20	
	Latent Dim	64	
	Cross Attention Heads	1	
	Latent Self-Attention Heads	8	
	Cross Head Dim	64	
	Latent Head Dim	64	
	Num Latent Blocks Per Layer	1	
Multimodal Cross-Attention Layer	Depth	1	
	Num Latents	20	
	Latent Dim	64	
	Cross Attention Heads	1	
	Latent Self-Attention Heads	8	
	Cross Head Dim	64	
	Latent Head Dim	64	
	Num Latent Blocks Per Layer	1	
Classification Heads (BatchNorm+Linear)	Input/output dimensions	756/32	1280/1
	Optimizer	Adam	
	Learning rate	0.0005	
	Weight decay	0.0	
	Training loss weights	100.0	1.0
	Batchsize	18	64
	Evaluation weights	100.0	1.0
Training	Original MultiBench Input Dimensions	Gripper Pos: 16x3 Gripper Sensors: 16x7 Image: 16x32x32 Control: 16x7	Image: 128x128x3 Force: 6x32 Proprio: 8 Depth: 128x128 Action: 4
	Perceiver Input Channel Size	Gripper Pos: 3 Gripper Sensors: 7 Image: 1 Control: 7	Image: 3 Force: 32 Proprio: 8 Depth: 1 Action: 4
	Perceiver Input Extra Axis	Gripper Pos: 1 Gripper Sensors: 1 Image: 3 Control: 1	Image: 2 Force: 1 Proprio: 1 Depth: 2 Action: 1
	Perceiver Input Num_freq_bands	Gripper Pos: 6 Gripper Sensors: 6 Image: 6 Control: 6	Image: 6 Force: 6 Proprio: 6 Depth: 6 Action: 6
	Perceiver Input Max_freq	Gripper Pos: 1 Gripper Sensors: 1 Image: 1 Control: 1	Image: 1 Force: 1 Proprio: 1 Depth: 1 Action: 1
	Shared Modality Encoding	N/A	

Table 9. Table of hyperparameters for multitask prediction on the **medium** setting involving AV-MNIST, ENRICO and PUSH: 3 tasks across 3 domains (multimedia, HCI, and affective computing), again with vastly different modality sets: {image, audio}, {image, set}, and {image, force, proprioception, control} for each task.

Part of Model	Hyperparameter	Values		
		AV-MNIST	ENRICO	PUSH
Unimodal Perceiver Encoder	Depth		1	
	Num Latents		12	
	Latent Dim		64	
	Cross Attention Heads		1	
	Latent Self-Attention Heads		8	
	Cross Head Dim		64	
	Latent Head Dim		64	
	Num Latent Blocks Per Layer		1	
Multimodal Cross-Attention Layer	Depth		1	
	Num Latents		12	
	Latent Dim		64	
	Cross Attention Heads		1	
	Latent Self-Attention Heads		8	
	Cross Head Dim		64	
	Latent Head Dim		64	
	Num Latent Blocks Per Layer		1	
Classification Heads (BatchNorm+Linear)	Input/output dimensions	128/10	128/20	768/2
	Optimizer		Adam	
	Learning rate		0.001	
	Weight decay		0.0	
	Training loss weights	0.8	1.0	1.1
	Batchsize	32	32	32
	Evaluation weights	1	1	1
Training	Original MultiBench Input Dimensions	Colorless Image: 28x28 Audio Spectrogram: 112x112	Image: 256x128x3 Set: 256x128x3	Gripper Pos: 16x3 Gripper Sensors: 16x7 Image: 16x32x32 Control: 16x7
	Perceiver Input Channel Size	Colorless Image: 16 (cut into 4x4 squares) Audio Spectrogram: 256 (cut into 16x16 squares)	Image: 3 Set: 3	Gripper Pos: 3 Gripper Sensors: 7 Image: 1 Control: 7
	Perceiver Input Extra Axis	Colorless Image: 2 Audio Spectrogram: 2	Image: 2 Set: 2	Gripper Pos: 1 Gripper Sensors: 1 Image: 3 Control: 1
	Perceiver Input Num_freq_bands	Colorless Image: 6 Audio Spectrogram: 6	Image: 6 Set: 6	Gripper Pos: 6 Gripper Sensors: 6 Image: 6 Control: 6
	Perceiver Input Max_freq	Colorless Image: 1 Audio Spectrogram: 1	Image: 1 Set: 1	Gripper Pos: 1 Gripper Sensors: 1 Image: 1 Control: 1
	Shared Modality Encoding	N/A		

Table 10. Table of hyperparameters for multitask prediction on the **large** setting involving MIMIC, AV-MNIST, MOSEI and UR-FUNNY: 4 tasks across 3 domains (healthcare, multimedia, and affective computing), again with vastly different modality sets: {time-series, table}, {image, audio}, and {text, video, audio} for the final 2 tasks with different format of preprocessed embeddings of video and audio.

Part of Model	Hyperparameter	Values			
		MIMIC	AV-MNIST	MOSEI	UR-FUNNY
Unimodal Perceiver Encoder	Depth		1		
	Num Latents		20		
	Latent Dim		64		
	Cross Attention Heads		1		
	Latent Self-Attention Heads		6		
	Cross Head Dim		64		
	Latent Head Dim		64		
	Num Latent Blocks Per Layer		1		
Multimodal Cross-Attention Layer	Depth		1		
	Num Latents		20		
	Latent Dim		64		
	Cross Attention Heads		4		
	Latent Self-Attention Heads		6		
	Cross Head Dim		64		
	Latent Head Dim		64		
	Num Latent Blocks Per Layer		1		
Classification Heads (BatchNorm+Linear)	Input/output dimensions	128/2	128/10	384/2	384/2
Training	Optimizer		Adam		
	Learning rate		0.0008		
	Weight decay		0.001		
	Training loss weights	1.2	0.9	1.1	1.5
	Batchsize	20	40	32	32
	Evaluation weights	1	1	1	1
	Original MultiBench Input Dimensions	Static: 5 Timeseries: 24x12	Colorless Image: 28x28 Audio Spectrogram: 112x112	Image: 50x35 Audio: 50x74 Text: 50x300	Image: 20x371 Audio: 20x81 Text: 50x300
	Perceiver Input Channel Size	Static: 1 Timeseries: 1	Colorless Image: 16 (cut into 4x4 squares) Audio Spectrogram: 256 (cut into 16x16 squares)	Image: 35 Audio: 74 Text: 300	Image: 371 Audio: 81 Text: 300
	Perceiver Input Extra Axis	Static: 1 Timeseries: 2	Colorless Image: 2 Audio Spectrogram: 2	Image: 1 Audio: 1 Text: 1	Image: 1 Audio: 1 Text: 1
	Perceiver Input Num_freq_bands	Static: 6 Timeseries: 6	Colorless Image: 6 Audio Spectrogram: 6	Image: 3 Audio: 3 Text: 3	Image: 3 Audio: 3 Text: 3
	Perceiver Input Max_freq	Static: 1 Timeseries: 1	Colorless Image: 1 Audio Spectrogram: 1	Image: 1 Audio: 1 Text: 1	Image: 1 Audio: 1 Text: 1
	Shared Modality Encoding	The text modality from MOSEI and UR-FUNNY are shared.			

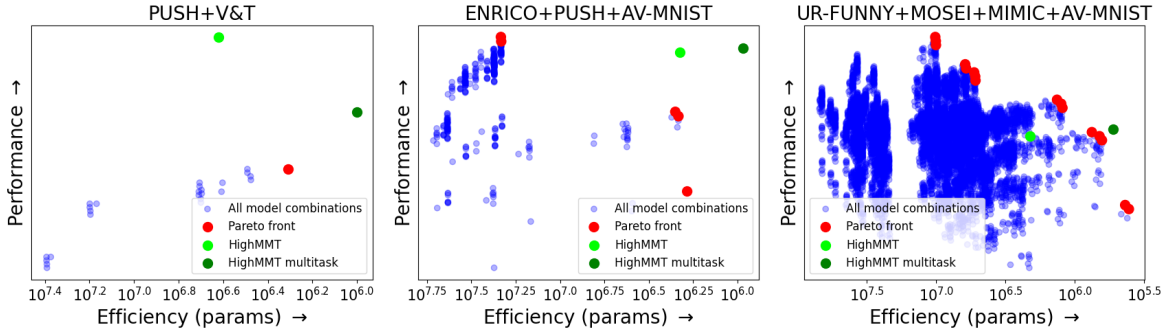


Figure 8. **Overall tradeoff** across the small (PUSH, V&T), medium (ENRICO, PUSH, AV-MNIST), and large (UR-FUNNY, MOSEI, MIMIC, AV-MNIST) multitask training settings. Multitask HIGHMMT pushes forward the Pareto front of performance and efficiency as compared to all possible ($> 10^5$) combinations of task-specific models across multiple datasets (Liang et al., 2021b). The x -axis denotes (inverted) total parameters and y -axis denotes performance scaled to a 0 – 1 range before averaging across datasets.

C. Additional Results

In this section, we detail additional experimental results that support the multitask, transfer, and generalization capabilities of HIGHMMT.

C.1. Multitask performance and efficiency

Figure 8 provides a more detailed comparison to task-specific state-of-the-art models in terms of tradeoffs between performance and efficiency. The blue dots represent all possible combinations of task-specific models across multiple datasets (summarized in MultiBench (Liang et al., 2021b), $> 10^5$ total combinations) with their overall performance (scaled to a 0 – 1 range before averaging across datasets) and overall efficiency (inverted total number of parameters). The red dots represent the state-of-the-art Pareto front: points that are not strictly dominated in both performance and efficiency. We can see that in the small and medium settings, both HIGHMMT and its multitask version outperform current baselines in MultiBench (Liang et al., 2021b) while reducing parameters through multitask learning. In the large setting, HIGHMMT and its multitask version are competitive with respect to strong baselines in MultiBench. In all cases, multitask HIGHMMT pushes forward the Pareto front by improving both performance and efficiency, and performs similar to (and sometimes better than) its single-task version while reducing parameters.

C.2. Generalization to new modalities and tasks

HIGHMMT also offers opportunities to study whether we can *transfer* knowledge between completely different tasks and modalities. On the large setting, we first pretrained a model on 0/1/2/3 of the four tasks before fine-tuning on the fourth task only. We show these full results in Table 11. On all four target tasks, our proposed multitask pretraining and fine-tuning paradigm improves performance over single target-task training. Therefore, weights learned from other multimodal tasks indeed generalize well to new modalities and tasks. We further analyze this transfer learning phenomenon by studying the following research questions:

Effect of pretraining datasets. When we vary the number of pretraining datasets, we observe a consistent improvement on fine-tuned target task performance across all datasets. This effect is particularly pronounced on the UR-FUNNY target task, which shows the biggest improvement using pretrained parameters from 0 to 3 multitask datasets. This implies that HIGHMMT learns more generalizable multimodal features as more tasks are involved in multitask training.

Effect of target dataset size. We observed an inverse correlation between target task size and performance improvement: the smallest dataset, UR-FUNNY, benefited the most (+2.4%) from transfer learning. This implies that this multimodal pretraining-fine-tuning paradigm is useful for improving performance for low-resource target modalities and tasks.

Effect of transfer modalities. We compare transfer learning performance across different levels of partial observability. While one would expect transfer to the MIMIC dataset to be the hardest due to its modality set {time-series, table} being completely disjoint from the remaining 3 datasets, we still observe a +0.8% gain as compared to single-task training. Therefore, HIGHMMT can generalize to new modalities and tasks. Unsurprisingly, for datasets with more overlap in modality sets (e.g., UR-FUNNY with complete overlap in {text, video, audio} as compared to the other 3 datasets used for

Table 11. We train multitask HIGHMMT on 1/2/3 datasets and find that it generalizes to new modalities and tasks on the 4th dataset, with improved performance over single-task training on the 4th dataset. 0 source tasks implies transferring randomly initialized parameters, which is equivalent to single-task training on the target task. Cross-modal transfer improves with the number of pretraining tasks and works best on the smallest target tasks (UR-FUNNY).

Source tasks	Target task UR-FUNNY
0 (no transfer)	63.3
MOSEI	64.1
MOSEI + AV-MNIST	65.5
MOSEI + MIMIC + AV-MNIST	65.7

Source tasks	Target task MOSEI
0 (no transfer)	79.4
AV-MNIST	79.4
AV-MNIST + MIMIC	80.0
UR-FUNNY + MIMIC + AV-MNIST	80.5

Source tasks	Target task MIMIC
0 (no transfer)	67.7
MOSEI	68.3
AV-MNIST + MOSEI	68.5
UR-FUNNY + MOSEI + AV-MNIST	68.5

Source tasks	Target task AV-MNIST
0 (no transfer)	70.4
MOSEI	70.4
MIMIC + MOSEI	70.5
UR-FUNNY + MOSEI + MIMIC	70.5

Table 12. Multitask HIGHMMT also enables training a single model for both multimodal fusion and retrieval tasks.

Model	AV-MNIST ↑	CIFAR-ESC ↑	Params (M) ↓
HIGHMMT	70.4	58.8	1.04
HIGHMMT multitask	70.4	60.5	0.52

pretraining, we find larger improvements using transfer learning over single-task models (+2.4%).

Comparisons to unimodal transfer. Recent work has explored the possibility of transferring Transformer representations trained in one modality to another. Lu et al. (2021) found that a frozen pretrained Transformer on text surprisingly transfers to a variety of sequence classification tasks of different modalities spanning numerical computation, vision, and protein fold prediction. This observation had been previously observed in transfer learning from language to vision (Kiela et al., 2019), referential communication games to real-world NLP tasks (Li et al., 2020), computational primitives to transfer to mathematics tasks (Wu et al., 2021), and between code, different languages, and music (Papadimitriou and Jurafsky, 2020). Our transfer experiments also corroborate these findings in a multimodal setting with promising results on new modalities and tasks, especially involving real-world, smaller, and noisier datasets such as those involving human videos (MOSEI and UR-FUNNY), medical data (MIMIC), or real and simulated robots (PUSH and V&T).

C.3. Multitask fusion and retrieval

To assess task generalization, we train multitask models over fusion in AV-MNIST and retrieval in CIFAR-ESC. While fusion emphasizes information integration from complementary data sources, retrieval focuses on aligning corresponding elements expressed through different views of the data (Baltrušaitis et al., 2018). Table 12 shows the full results of this experiment: even across vastly different multimodal prediction tasks, we find that multitask training (60.5% retrieval accuracy) improves upon single-task training (58.8% accuracy), while performance on the AV-MNIST fusion tasks is similar for both single-task and multitask learning. Not only have the unimodal encoders simultaneously processed different modalities, the multimodal attention layer has also learned to capture correspondences useful for both fusion and retrieval, while halving the total number of parameters required as compared to task-specific modeling.

Table 13. **Ablation studies** show that removing any of the 4 components in HIGHMMT results in worse overall performance, and separating rather than sharing parameters also reduces performance while introducing more parameters. Note that HIGHMMT multitask w/o unimodal actually introduces more parameters, since Crossmodal Transformer layers increase in size to directly operate on large input data dimensions rather than small latent vector dimensions when Perceiver unimodal encoders are removed.

Model	UR-FUNNY	↑MOSEI	↑MIMIC	↑AV-MNIST	↑Ave	↑Params (M) ↓
HIGHMMT multitask	63.0	79.9	67.8	70.4	70.3	0.53
- w/o embeddings	62.5	78.4	67.9	69.5	69.6	0.52
- w/o unimodal	57.6	61.8	63.0	59.1	60.4	5.31
- w/o multimodal (Jaegle et al., 2021b; Likhoshesterov et al., 2022)	61.3	80.3	67.7	69.4	69.7	0.28
- separate (Tsai et al., 2019; Hendricks et al., 2021)	63.4	79.7	68.5	69.0	70.2	3.25
- separate unimodal	64.6	79.9	65.4	69.3	69.9	2.59
- separate multimodal	63.5	79.5	65.3	70.0	69.6	1.31

C.4. Understanding HIGHMMT

In this subsection, we analyze why this general model achieves strong results in multitask, transfer, and few-shot settings. Based on prior work in multitask learning (Caruana, 1997; Ruder, 2017; Zhang and Yang, 2021), we set up two possible hypotheses: (1) improved generalization and (2) improved regularization. We supplement the results in the main paper with additional visualizations and comparisons in this subsection.

C.4.1. HYPOTHESIS 1: IMPROVED GENERALIZATION

Investigating parameter sharing. In which components of the HIGHMMT model is parameter sharing important?

We further study the importance of parameter sharing in HIGHMMT. From the ablation studies in Table 13, using separate parameters for either unimodal or multimodal layers results in worse performance. The full model with completely separate unimodal and multimodal layers is reminiscent of typical single-task multimodal transformers (Tsai et al., 2019; Lu et al., 2019; Hendricks et al., 2021) trained separately for each task. We show that HIGHMMT maintains competitive performance (with slightly better performance on several datasets) due to statistical strength sharing, while also reducing parameters by 6× due to sharing of unimodal encoders and multimodal layers across tasks.

Furthermore, we surprisingly find that removing the modality-specific embedding layer results in only slightly worse performance (70.3 to 69.6 average score). This implies that the shared unimodal encoder has learned generalizable feature extractors that can encode heterogeneous modalities even without a modality identifier.

Visualization of attention patterns. How do the shared unimodal encoders attend to modality-specific tokens?

Given that parameter sharing seems to be useful for performance and efficiency, we aim to better visualize the nature of information sharing in the attention layers of unimodal encoders. We perform inference on a trained multitask HIGHMMT model on the test data of the large multitask setting, and average the attention patterns across test datapoints for each dataset. Following Lu et al. (2021), the average attention pattern provides information on general inductive biases captured by the unimodal encoders and enables us to make holistic conclusions rather than comparing attention maps on individual datapoints.

From Figure 9, we actually find that a common attention pattern emerges across modalities and tasks. First looking across modalities in the same dataset, we find that the model captures common temporal patterns at the same time steps, which makes sense since the 3 modalities are time-aligned in a video. The attention patterns are quite similar which implies that the same attention strategy can often work well across different modalities and tasks. This could be an explanation of why our model is able to perform multiple tasks simultaneously using shared parameters in attention layers.

It is also interesting to see how the model automatically learns to “divide up work” amongst its 20 latent tokens (numbered 0-19): the latent tokens 10 – 13 typically all focus on the region about two-thirds after the start of the input sequence, while latent tokens 1 and 3 always focuses on the region about one-third from the start. Certain tokens (3 and 18) seem to learn oscillating attention patterns, and certain pairs of tokens learn complementary attention patterns (e.g., 4, 5, and 6 attend one after the other). There are also some latent tokens that more evenly attend to the whole input sequence, such as latent tokens 9 and 17, which can be seen as “summary” tokens. This shows that the perceiver-based encoder is able to divide up its limited latent space well to capture important information both in specific time-steps and contextual information across all the time-steps, thus creating a holistic representation of the input using a much smaller set of latent variables.

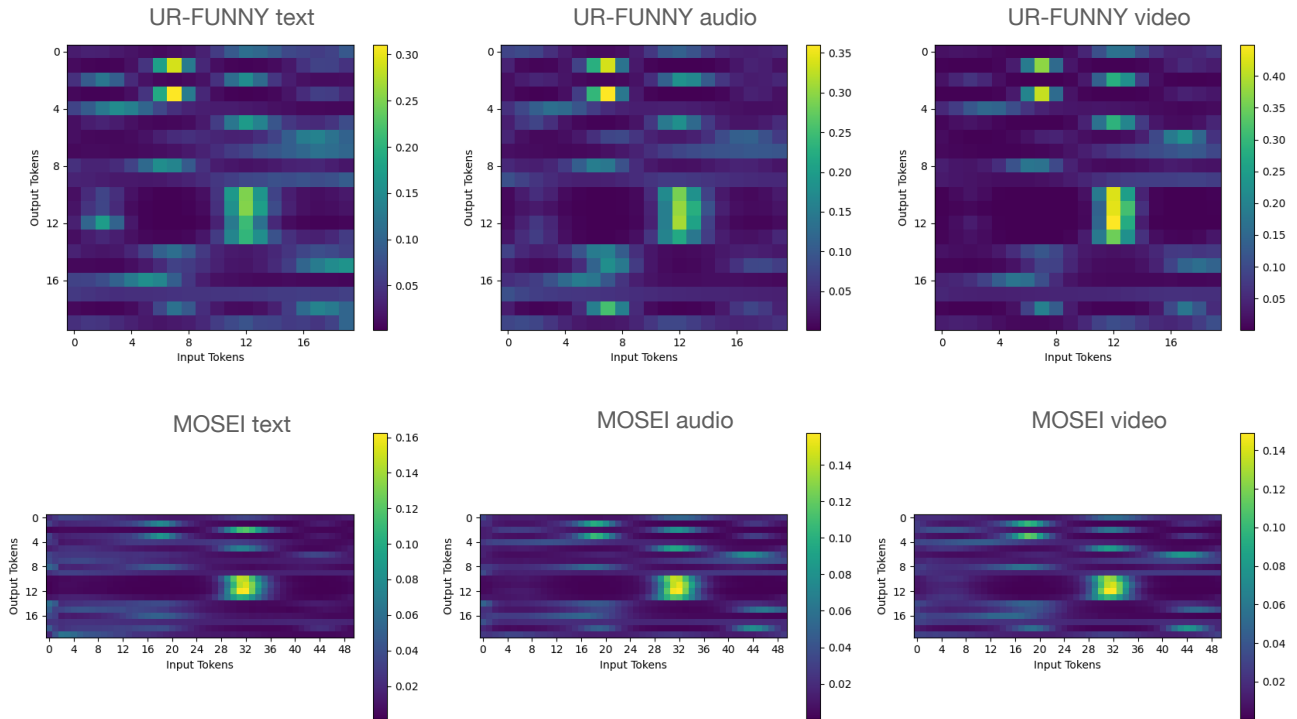


Figure 9. Visualizations of attention patterns learned by the unimodal encoders across different modalities and datasets. We find that there are some common attention patterns across tasks, which implies that the shared unimodal encoders have learned common information across tasks.

C.4.2. HYPOTHESIS 2: IMPROVED REGULARIZATION

In parallel to improved generalization, another line of research has focused on the regularization effects of multitask learning. Baxter (1997) showed that multitask parameter sharing reduces the risk of overfitting on the original task by forcing the model to learn across multiple tasks. We study the following regularization effects:

Training dynamics. In Figure 10, we traced the train and valid accuracies across 60 training epochs (with multitask training in the large setting). The training process of HIGHMMT converges at about the same rate between single-task and multitask learning, but the multitask model overfits less (a smaller gap between training and valid accuracies). This implies that multitask training helps to regularize the joint parameters and alleviates their overfitting on the target task.

Task weights. We found that optimizing a simple weighted sum of loss functions over all tasks was sufficient to obtain strong multitask performance. Instead of assigning uniform weights to each task, sometimes we found it helpful to set the weight higher for more challenging datasets during HIGHMMT multitask training. We show some examples of this phenomenon in Figure 11, where multitask performance can sometimes be sensitive to weights especially when prediction

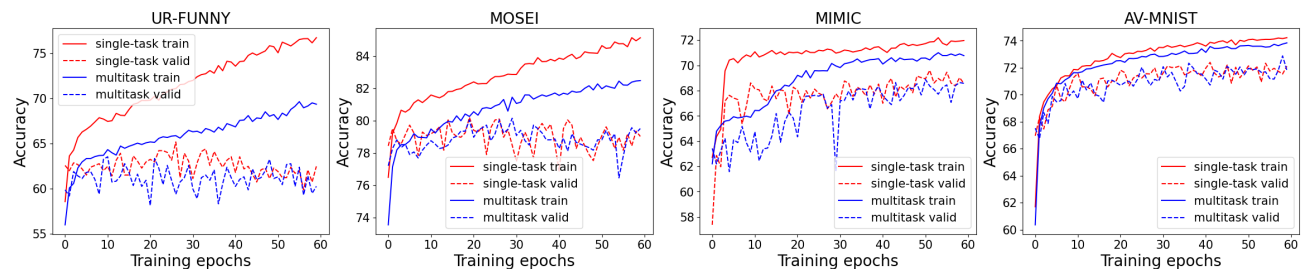


Figure 10. Multitask models converge as fast but overfit less (a smaller gap between train and valid accuracies) vs single-task models, which implies that multitask training helps to regularize the joint parameters and reduces overfitting on the target task.

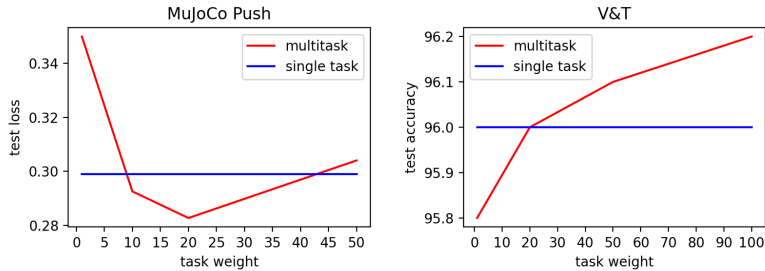


Figure 11. Multitask performance can sometimes be sensitive to task weights especially when prediction objectives are of different scales (i.e., MSE for PUSH vs accuracy for V&T), in a manner similar to how carefully-tuned regularization terms help in training models.

objectives are of different scales (i.e., MSE vs accuracy). This supports the regularization argument where carefully tuned weighted auxiliary objectives encouraging the model to also fit other auxiliary tasks can help improve performance on a target task. However, doing so would not achieve the best performance on auxiliary tasks.

C.5. Summary of main take-away messages

In conclusion, we designed a general multimodal multitask model for high-modality (a large set of diverse modalities) and partially-observable (each task only defined on a small subset of modalities) scenarios. Our approach relies on training for *multitask* and *transfer* learning: multitask learning with shared unimodal and multimodal layers enables stable parameter counts (addressing scalability) and cross-modal transfer learning enables information sharing across modalities and tasks (addressing partial observability). Through an extensive set of experiments and analysis, we summarize our main take-away messages as follows:

1. **Standardized multitask modeling.** We train a single multitask HIGHMMT model for numerous high-modality and partially-observable multimodal tasks (across 10 modalities, 15 prediction tasks, and 5 research areas), achieving strong performance while reducing total parameter counts. We believe that standardized modeling leads to a smaller set of architectural decisions, enables transfer to understudied modalities and tasks, and present a unified platform for subsequent theoretical and empirical analysis.
2. **Cross-modal transfer to new modalities and tasks.** Multitask HIGHMMT enables cross-modal information transfer by pretraining on source multimodal tasks before transferring to completely new target modalities and tasks. Involving more tasks during pretraining improves performance, and gains are more apparent when fine-tuning on low-resource target tasks. This finding can supplement current pretrain-finetune paradigms typically performed on the same modality (e.g., text-only or image-only), and encourage research in more general multimodal pretraining over high-modality settings before fine-tuning on only a partial subset of all observed modalities.
3. **Tradeoff between performance and efficiency.** Multitask HIGHMMT improves the tradeoff between performance and efficiency over task-specific state-of-the-art models especially in low-resource scenarios (less training data and partially-observable modalities). Coupled with the relatively fewer architectural decisions and generalization to understudied modalities and tasks, we believe that multitask HIGHMMT and similar architectures should be a starting point for future research.
4. **Few-shot multitask learning.** Multitask information sharing can improve performance on low-resource target tasks with limited labeled training data. Therefore, if it is too difficult to collect data in a target domain, collecting data from a different domain and using a shared multimodal model is an alternative approach for improving performance.
5. **Information sharing.** Finally, our analysis reveals surprising insights regarding the nature of information sharing in multimodal and multitask models, which may be of independent interest. Specifically, there are both generalization and regularization effects at play in our implementation of multimodal multitask learning:
 - On the generalization side, information sharing is present across modalities and tasks, but at different levels across shared unimodal and multimodal layers. Information sharing enables strong multitask performance even under partial-observability and generalization to new modalities and tasks via transfer learning.

HIGHMMT: Towards Modality and Task Generalization for High-Modality Representation Learning

- While using modality-specific embeddings achieves best performance, there is only a minor drop when removing them, which implies that shared unimodal encoders can learn generalizable feature extractors even without a modality identifier.
- On the regularization side, well-tuned regularization weights yield training dynamics that display less overfitting on target tasks as compared to single-task learning.